Dark carbon fixation in the Arabian Sea oxygen minimum zone contributes to sedimentary organic carbon (SOM)

Sabine K. Lengger[1,2,3*], Darci Rush[3], Jan Peter Mayser[2], Jerome Blewett[2], Rachel Schwartz-Narbonne[4], Helen M. Talbot[4,†] , Jack J. Middelburg[5], Mike S.M. Jetten[6], Stefan Schouten[3,5], Jaap S. Sinninghe Damsté[3,5] and Richard D. Pancost[2]

[1] Biogeochemistry Research Centre, School of Geography, Earth and Environmental Science, University of Plymouth, PL48AA, Plymouth, United Kingdom.

[2] Organic Geochemistry Unit, School of Chemistry, University of Bristol, BS81TS, Bristol, United Kingdom.

[3] NIOZ Royal Netherlands Institute for Sea Research, Dept. of Marine Microbiology and Biogeochemistry, and Utrecht University,1797SZ, Texel, The Netherlands.

[4] School of Natural and Environmental Sciences, Newcastle University, Drummond Building, NE1 7RU, Newcastle-upon-Tyne, United Kingdom.

[5] Department of Earth Sciences, Faculty of Geosciences, Utrecht University, 3508 TA, Utrecht, The Netherlands.

[6] Department of Microbiology, IWWR, Radboud University Nijmegen, 6525 XZ, Nijmegen, The Netherlands

* corresponding author: Sabine Lengger (sabine.lengger@plymouth.ac.uk)

† present address: BioArCh, Environment Building, University of York, YO10 5DD, Heslington, United Kingdom.

Key Points:

- One fifth of organic matter on Arabian Sea seafloor could stem from bacterial carbon fixation in the oxygen minimum zone

- Evaluation of past anoxic events needs to take chemoautotrophic contribution into account in isotope balances

- Biogeochemical models ignoring dark carbon fixation could highly underestimate oxygen demand and thus expansion of oxygen minimum zones

Abstract

In response to rising CO_2 concentrations and increasing global sea surface temperatures, oxygen minimum zones (OMZ), or "dead zones", are expected to expand. OMZs are fueled by high primary productivity, resulting in enhanced biological oxygen demand at depth, subsequent oxygen depletion, and attenuation of remineralization. This results in the deposition of organic carbon-rich sediments. Carbon drawdown is estimated by biogeochemical models; however, a major process is ignored: carbon fixation in the mid- and lower water column. Here, we show that chemoautotrophic carbon fixation is important in the Arabian Sea OMZ; and manifests in a ^{13}C-depleted signature of sedimentary organic carbon. We determined the $\delta^{13}C$ values of SOM deposited in close spatial proximity but over a steep bottom-water oxygen gradient, and the $\delta^{13}C$ composition of biomarkers of chemoautotrophic bacteria capable of anaerobic ammonia oxidation (anammox). Isotope mixing models show that detritus from anammox bacteria or other chemoautotrophs likely forms a substantial part of the organic matter deposited within the Arabian Sea OMZ (~17%), implying that the contribution of chemoautotrophs to settling organic matter is exported to the sediment. This has implications for the evaluation of past, and future, OMZs: biogeochemical models that operate on the assumption that all sinking organic matter is photosynthetically derived, without new addition of carbon, could significantly underestimate the extent of remineralization. Oxygen demand in oxygen minimum zones could thus be higher than projections suggest, leading to a more intense expansion of OMZs than expected.

Plain Language Summary

Oxygen minimum zones are areas in the ocean in which algae produce large amounts of organic material. When this sinks towards the seafloor, all oxygen at depth is used up. This results in vast "dead zones" where almost no oxygen is available to sustain life. With global warming, and increased nutrients from rivers, dead zones are forecast to expand. Computer models can calculate this, by considering algal production, and the amount of material delivered to the seafloor. However, these models often ignore a major process: anaerobic bacteria in the deeper water column, that can live at the edge or in the middle of these dead zones, which can also produce organic material from the dissolved CO_2. In this study, we used the fact that these bacteria add a distinct signature to the organic material, to show that one fifth of the organic matter on the seafloor could stem from bacteria living in these dead zones. Thus, models that have missed out on considering this contribution could have underestimated the extent of oxygen depletion we are to expect in a future, warming world. A more intense expansion of dead zones than expected could have severe ecological, economical (fisheries), and climatic consequences.

64   1 **Introduction**

65   Marine primary production fixes 50 Pg carbon per year, of which only about 1% is buried
66   in sediments (Dunne et al., 2007; Middelburg, 2011). The majority of organic carbon derived
67   from the photic zone is remineralised during sedimentation, fueling heterotrophic bacterial
68   activity in the water column (Keil et al., 2016). In marginal settings and OMZs, marine primary
69   production in the photic zone can be significantly higher than in other settings. Organic carbon
70   (OC) sedimentary accumulation rates within an OMZ can be in the range of tens to hundreds of
71   mg C cm^{-2} y^{-1} (Hartnett et al., 1998; Hedges and Keil, 1995) higher than observed in other parts
72   of the ocean. These high accumulation rates are most commonly attributed to attenuation in
73   remineralization rates within the OMZ, and low bottom-water oxygenation, which results in
74   decreased biodegradability of polymeric and matrix-protected substances (Burdige, 2007).

75   As a consequence of increasing atmospheric CO_2 concentrations and, consequently,
76   temperature, oceanic OMZs are forecast to expand in a fashion similar to the past (Breitburg et
77   al., 2018; Queste et al., 2018; Schmidtko et al., 2017; Shaffer et al., 2009; Stramma et al., 2010).
78   Whilst the expansion of OMZs will result in widespread habitat loss of marine life and could
79   cause an increase in emissions of greenhouse gases such as N_2O and CH_4, it could also act as a
80   long-term negative feedback on global warming via the enhanced drawdown and storage of
81   organic carbon in sediments.

82   The biogeochemical system in subsurface waters, where light does not penetrate, has
83   recently emerged to be substantially more complex – and possibly more important for the global
84   carbon cycle – than previously assumed. In particular, dark water-column microbial activity is
85   higher than what can be accounted for by heterotrophs (Herndl and Reinthaler, 2013), suggesting
86   an important role for chemoautotrophy, i.e. fixation of dissolved inorganic carbon (DIC). It has
87   been suggested to contribute substantially to the global carbon budget, with estimates ranging
88   from 0.11 to 1.1 Pg C y^{-1}, equating to ca. 2% of total estimated yearly marine primary production
89   (Middelburg, 2011; Reinthaler et al., 2010). The predominant chemoautotrophic process in the
90   oxic, dark, pelagic ocean is thought to be nitrification (Middelburg, 2011; Pachiadaki et al.,
91   2017). When oxygen is limited, nitrification still occurs, but other chemoautotrophic processes
92   dominate, such as anaerobic oxidation of ammonia and sulfide oxidation (Ulloa et al., 2012;
93   Wright et al., 2012).

94   Under hypoxic conditions, such as in the water column of OMZs, both archaeal (aerobic)
95   and anaerobic oxidation of ammonia are thought to dominate dark inorganic carbon fixation
96   processes (Lam and Kuypers, 2010; Pitcher et al., 2011). Here, nitrite accumulates, and other
97   anaerobic autotrophic processes such as sulfide oxidation and methanogenesis are suppressed,
98   most likely due to the abundance of nitrate and ammonia (Canfield, 2006; Ulloa et al., 2012).

99   Of the inorganic carbon converted to organic matter within the OMZ, only a negligible
100 fraction is presumably transported to the sediments and preserved, as this newly produced
101 material is regarded as more labile than the sinking OC derived from the photic zone (Cowie and
102 Hedges, 1992; Keil et al., 1994; Middelburg, 1989). Dark carbon fixation rates are challenging to
103 quantify: they have been determined experimentally (Reinthaler et al., 2010; Taylor et al., 2001),
104 or have been estimated from the reaction stoichiometry of respiration based on Redfield organic
105 matter and growth yields of nitrifiers (Middelburg, 2011; Wuchter et al., 2006). In OMZs, such
106 as the Peruvian margin (Lam et al., 2009), the Arabian Sea (Jensen et al., 2011), or the sulfidic
107 Black Sea (Lam et al., 2007), the activity of some chemoautotrophs was determined via [15]N-

108 labelling, and formation of the products of their biogeochemical reactions. However, incubation
109 methods may suffer from bias, because *in situ* conditions such as pressure are difficult to
110 maintain.

111 However, carbon from within anoxic waters has been observed in some settings to
112 contribute to the particulate OC flux: for example, in eutrophic lakes (Hollander and Smith,
113 2001) and anoxic fjords (van Breugel et al., 2005b). Furthermore, discrepancies between
114 modelled and observed organic carbon fluxes suggest that dark carbon fixation in anoxic marine
115 settings significantly contributes to sinking material (Keil et al., 2016; Taylor et al., 2001).

116 One way to constrain this input into sedimentary organic matter is to use isotope mixing
117 models. Photosynthetically fixed carbon generally has stable carbon isotopic compositions of ca
118 -19 to -21 ‰ due to Rubisco fixation. However, chemoautotrophs dwelling in OMZs typically
119 have a lower $\delta^{13}C$ values. This is the result of multiple factors: they either use ^{13}C-depleted CO_2
120 generated by remineralization, have larger fractionation factors due to the higher abundance of
121 CO_2 at depth (Freeman et al., 1994), or use carbon fixation pathways such as the acetyl
122 coenzyme A pathway, which results in ^{13}C-depleted biomass (Hayes, 2001). This characteristic
123 chemoautotrophic isotopic signature in the organic carbon could allow us to quantify the
124 contribution of dark carbon fixation to sedimentary organic matter.

125 Here, we investigated the $\delta^{13}C$ value of sedimentary organic matter of surface sediments
126 deposited within the OMZ of the Arabian Sea and employed a simple isotope mixing model to
127 investigate the extent of input from OMZ carbon fixation into sedimentary organic matter. As the
128 major process in the Arabian Sea OMZ known to produce isotopically light biomass is anaerobic
129 oxidation of ammonia (anammox; Ulloa et al., 2012; Villanueva et al., 2014), in order to
130 determine the isotopic signature of this pathway, we developed and applied a method to
131 determine the $\delta^{13}C$ values of a novel biomarker, bacteriohopanetetrol stereoisomer (BHT'),
132 which has been found to be unique to anammox bacteria in the marine environment in culture
133 and environmental studies (Rush et al., 2014, 2019; Rush and Sinninghe Damsté, 2017). It has
134 been found in the Arabian Sea and other marine anoxic settings (Matys et al., 2017; Sáenz et al.,
135 2011). We also used stable isotope probing experiments to exclude sedimentary anammox as an
136 important contributor to this process. This allowed us to investigate the contribution of these
137 dark carbon fixers to sedimentary organic carbon.

138 **2   Materials and Methods**

139 2.1 Sediment sampling and stable isotope probing incubations

140 Sediments were collected with multicore devices on the R/V Pelagia in the Northern
141 Arabian Sea in January 2009 during the PASOM cruise 64PE301 along the Murray Ridge (Fig.
142 1f), which protrudes into the core of the OMZ. Two cores, one each from P900 (885 m water
143 depth) and P1800 (1786 m water depth), hereinafter referred to as anoxic and oxic, respectively,
144 were incubated on board as described by Pozzato et al. (2013 a, b). In brief, particulate or
145 dissolved organic matter from the diatom *Thalassiosira pseudonana* containing 20 and 18 % ^{13}C,
146 respectively, were added to the tops of core tubes of 10 cm internal diameter. Between 2 and 6 %
147 of the added carbon was respired, resulting in a highly enriched $^{13}C_{DIC}$ pool, enabling the tracing
148 of autotrophic processes in addition to heterotrophic processes.

149
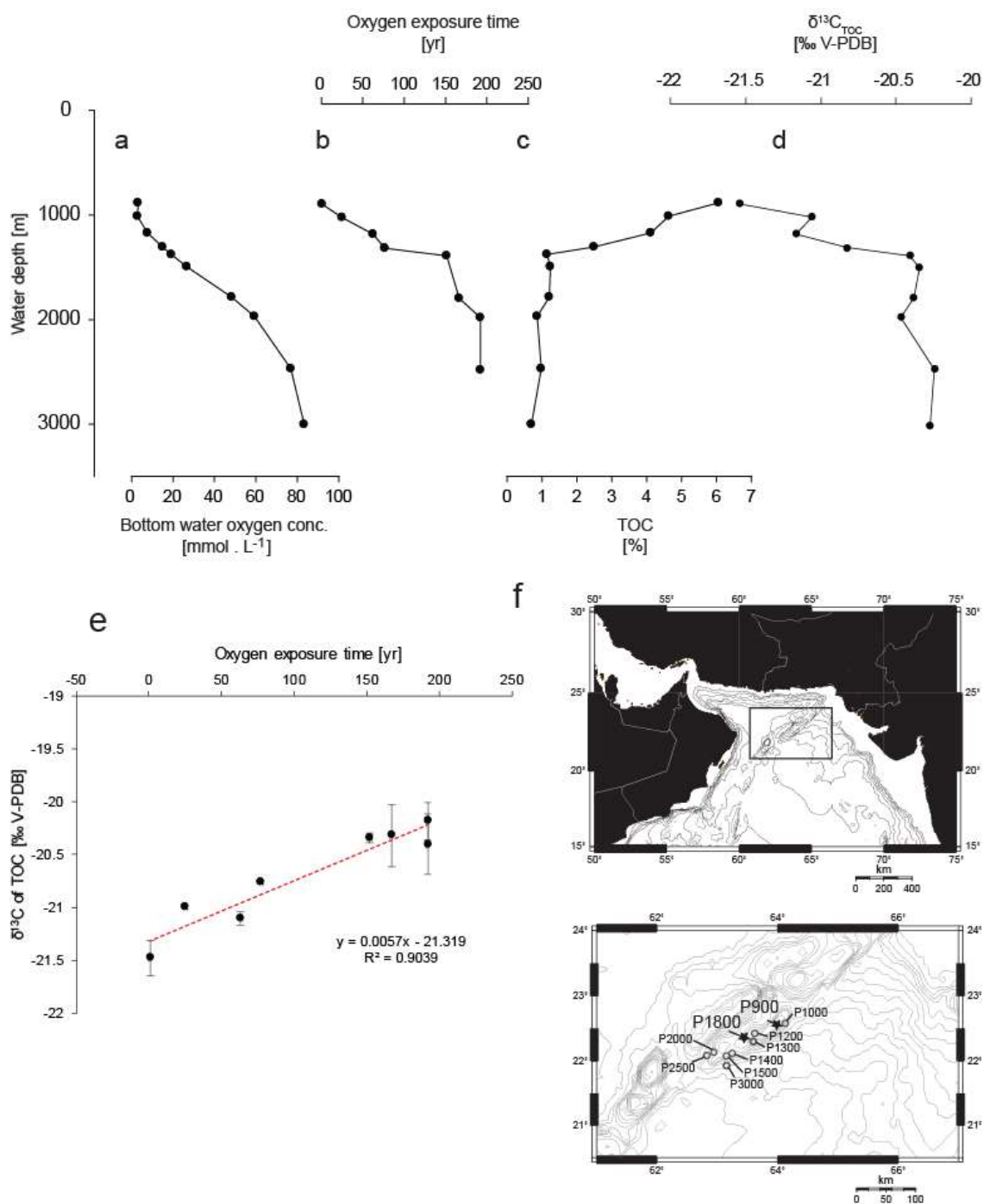
Figure 1. Arabian Sea depth gradients. Shown are $\delta^{13}C_{org}$ and % TOC values of core top sediments, and bottom water oxygenation plotted with depth (a-d), all but $\delta^{13}C_{org}$ replotted from Lengger et al. (2014), a scatter plot of oxygen exposure time versus $\delta^{13}C_{org}$ in Arabian Sea core tops along Murray Ridge (e), and a map of the sampling stations with the two main stations used for BHT analysis used here indicated with a star (f).

157   Eight cores are discussed here; these were incubated under oxic or suboxic conditions for
158 7 days (125 μM, 6 μM O_2, respectively; Table 1). At the end of incubation, cores were sliced in
159 the intervals 0 – 2, 2 – 4, and 4 – 10 cm depth. They were then frozen and freeze dried for the
160 isotopic analysis of the bacteriohopanepolyol lipids (BHPs), including bacteriohopanetetrol
161 (BHT) and its stereoisomer and biomarker for anammox bacteria, BHT'. Both biomarkers have
162 been studied previously in the Arabian Sea water column and sediments (Jaeschke et al., 2009;
163 Sáenz et al., 2011) Furthermore, cores from 8 stations between 900 and 3000 m water depth were
164 also collected, as described by Lengger et al. (2014, 2012b). The top 0 – 0.5 cm were used for
165 total organic carbon (TOC) and ^{13}C of organic carbon analysis. For the core from P900 (32 cm
166 length), all depths were analysed in 0.5 cm – 4 cm resolution (Lengger et al., 2012b).

167 2.2   Anammox enrichment cultures

168   To determine the $\delta^{13}C$ values for the two bacteriohopanetetrols in anammox bacteria
169 (BHT and BHT', the latter being unique to anammox in the marine environment), an enrichment
170 culture of '*Ca.* Scalindua profunda' was analysed. It was grown in a sequencing batch reactor as
171 described by van de Vossenberg et al. (2008). Analysis of this enrichment culture that showed
172 '*Ca.* S. profunda' comprised about 80% of the cells, while other bacteria belonging to the phyla
173 Bacteriodetes (including Flavobacteriaceae) and Proteobacteria (including Alphaproteobacteria)
174 accounted for the majority of the remaining populations (van de Vossenberg et al., 2008, 2013).

175 2.3. Extraction and purification

176   The freeze-dried subsamples of the unamended and incubated cores were ground, and the
177 homogenised sediments and the culture were extracted by a modified Bligh-Dyer extraction
178 method (Lengger et al., 2012a). Briefly, they were extracted ultrasonically three times in a
179 mixture of methanol/dichloromethane (DCM)/phosphate buffer (2:1:0.8, v:v:v) and centrifuged,
180 and the solvent phases were combined. The solvent ratio was then adjusted to 1:1:0.9, v:v:v to
181 separate the DCM phase. Liquid extraction was repeated two more times, the DCM fractions
182 were combined, the solvent was evaporated and the larger particles were filtered out over glass
183 wool. The extraction procedure was performed on the enrichment culture material and repeated
184 on the sediment for analysis of BHPs. An aliquot of the extract was subjected to column
185 chromatography using 5% aminopropyl solid phase extraction (SPE), eluting with hexane, DCM,
186 and MeOH, which contained BHPs. For analysis by chromatographic techniques, the extract was
187 derivatised in 0.5 mL of a 1:1 (v:v) mixture of acetic anhydride and pyridine at 50 °C for 1 h,
188 then at room temperature overnight in the case of HPLC-MS analysis. Solvent was dried under a
189 stream of N_2 on a 50°C heating block.

190 2.4. Instrumental techniques

191 2.4.1. High temperature gas chromatography coupled to flame ionization detection (HTGC-FID)

192   GC analysis of acetylated BHPs was done using a HP-5890 Series II GC equipped with a
193 flame ionization detector was fitted with a 0.25 mm x 0.1 μm VF5-ht capillary column (CP9045,
194 CP9046, Agilent Technologies UK Ltd., Stockport, UK) of 30 m length (Lengger et al., 2018).
195 An on-column injector was used. To the 30 m column, 1m of a 0.25 mm HT-deactivated silica
196 tubing was attached as a guard column (Zebron Z-Guard, 7CG-G000-00GH0, Phenomenex,
197 Macclesfield, UK). Analysis of bacteriohopanepolyols employed a constant flow of 2 ml/min He
198 and a temperature ramp from 70°C (1 min hold) to 400°C at 7°C min^{-1} (1 min hold).

199
200

2.4.2. High temperature gas chromatography coupled to mass spectrometric detection (HTGC-MS)

201 Analysis of acetylated BHPs, using HTGC-MS was performed using a Thermo Scientific
202 Trace 1300 gas chromatograph coupled with an ISQ single quadrupole mass spectrometer.
203 Diluted samples were introduced using a PTV injector in splitless mode onto a 0.53 mm fused
204 silica pre-column connected to a 30 m × 0.25 mm i.d. fused-silica capillary column coated with
205 dimethyl polysiloxane stationary phase (ZB-5HT; film thickness, 0.1 μm; 7HG-G015-02,
206 Phenomenex, Macclesfield, UK). The initial injection port temperature was 70 °C with an
207 evaporation phase of 0.05 min, followed by a transfer phase from 70 °C to 400 °C at 0.2 °C s^{-1}.
208 The oven temperature was held isothermally for 1 min at 70 °C, increased at a rate of 7 °C min^{-1}
209 to 400 °C and held at 400 °C for 10 min. Helium was used as a carrier gas and maintained at a
210 constant flow of 2.5 ml min^{-1}. The mass spectrometer was operated in the electron ionization
211 (EI) mode (70 eV) with a GC interface temperature of 400 °C and a source temperature of
212 340 °C. The emission current was 50 μA and the mass spectrometry set to acquire in the range of
213 *m/z* 50–950 Daltons with 0.5 s dwell time. Data acquisition and processing were carried out
214 using the Thermo XCalibur software (version 3.0.63). Due to the lack of authentic standards for
215 BHT and BHT', only relative and not absolute values are reported, assuming similar ionization
216 energies.

217
218

2.4.3. High temperature gas chromatography coupled to isotope ratio mass spectrometry (HTGC-IRMS)

219 The stable carbon isotopic composition (δ^{13}C) of BHPs were determined using HTGC-
220 isotope ratio mass spectrometry. To this end, an Elementar visION IRMS with GC5 interface
221 (Elementar UK Ltd., Cheadle, UK), and an Agilent 7890B GC were modified in-house and
222 allowed us to achieve column temperatures of up to 400 °C, which resulted in baseline resolution
223 of BHT and BHT' (Fig. 2). 1 μl of the derivatized samples dissolved in ethyl acetate were
224 injected on a cool-on-column injector, into a Zebron Z-Guard Hi-Temp Guard Column (1 m x
225 0.25 mm, Zebron Z-Guard, 7CG-G000-00GH0, Phenomenex, Macclesfield, UK) and separated
226 on a Zebron ZB-5HT analytical column (30 m x 0.25 mm x 0.1 μm, Phenomenex Ltd.,
227 Macclesfield, UK). He was used as a carrier gas at a flow rate of 1.5 ml min^{-1} and the oven was
228 programmed as follows: 1 min hold at 70 °C, increase by 7 °C min^{-1} to 350 °C (10 min hold).
229 Organic compounds were combusted to CO_2 in a 0.7 mm ID quartz tube with CuO pellets at
230 850°C. Instrumentation performance was monitored using an n-alkane standard (B3, A.
231 Schimmelmann, Indiana University, Bloomington, IN, USA; RMS 0.4 ‰), and results were
232 calibrated using an in-house mixture of five fatty acid methyl esters, which was injected between
233 every six sample analyses and analyzed using a He flow of 1 ml min^{-1}, with a slightly different
234 temperature program (injection at 50 °C held for 1 min followed by an increase of 10°C min^{-1} to
235 300 °C and a 10 min hold). This is the first time baseline resolution between BHT and BHT' has
236 been achieved on a GC-IRMS, which allows the direct determination of the isotopic composition
237 of both BHT and BHT' in sediment samples (Fig. 2). The isotopic composition of the acetyl
238 group used to derivatise the BHT and BHT' was determined by acetylation of *myo*-inositol, and
239 then subtracted from the values of BHT and BHT' in a mass balance correction (Angelis et al.,
240 2012), as authentic standards for BHT or BHT' were not available.

241
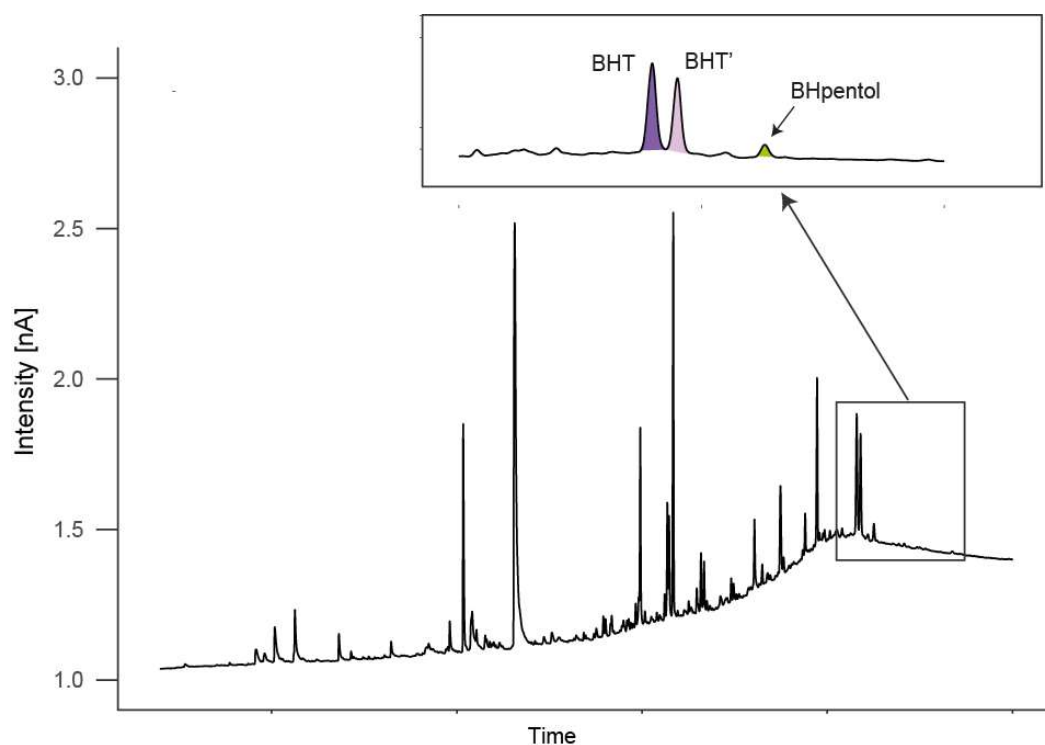
242
243 **Figure 2.** HTGC-IRMS chromatogram showing baseline separation between BHT, BHT', and
244 BHpentol.

245 2.4.4. High performance liquid chromatography coupled to positive ion atmospheric pressure
246 chemical ionization mass spectrometry (HPLC/APCI-MS)

247   To verify the GC-derived assignments, an aliquot of the acetylated BHP samples was
248 dissolved in MeOH:propan-2-ol (3:2; v:v) and filtered on 0.2 μm PTFE filters. BHPs were
249 analysed by HPLC/APCI-MS, using a data-dependent scan mode (3 events) on an HPLC system
250 equipped with an ion trap MS, as described in Talbot et al. (2007) and van Winden et al. (2012).
251 Relative BHP concentrations were semi-quantitatively estimated based on the response factor of
252 authentic standards (M. Rohmer; Strasbourg, France; Cooke et al., 2008), with a typical
253 reproducibility of ± 20%, according to Cooke et al. (2009).

254 2.4.5. Bulk sedimentary organic matter and suspended particulate matter

255   Freeze-dried core tops from 8 stations between 900 and 3000 m for sedimentary organic
256 matter, and punches from 0.7 μm GFF filters for suspended particulate organic matter, were
257 decalcified with 2N HCl, washed, freeze-dried, and subjected to analysis via a Flash EA 1112
258 Series (Thermo Scientific) analyser, coupled via a Conflo II interface to a Finnigan Delta[plus]
259 mass spectrometer as described by Lengger et al. (2014; sediment) and Pitcher et al. (2011;
260 filters). Standards for $\delta^{13}C$ analysis were acetanilide and benzoic acid and samples were analysed
261 in duplicate.

3. Results

To quantify the provenance of sedimentary organic matter and the contribution of anammox from the OMZ, we analysed the isotopic composition of sedimentary organic matter deposited in close spatial proximity over a large depth gradient in the Arabian Sea, as well as the isotopic composition of biomarker lipids derived from anammox bacteria, chemoautotrophic microbes living in the OMZ. In order to determine whether these were water-column derived or sedimentary, we used stable isotope probing experiments on sediments retrieved from within and below the OMZ.

3.1. $\delta^{13}C$ values of C_{org}

$\delta^{13}C$ values of C_{org} in surface sediments were low (-21.5 ‰) at P900 and increased with water depth to -20.2 ‰ at P2500 (Fig. 1d). $\delta^{13}C_{org}$ values correlated positively and linearly (Slope 0.0057, $R^2 = 0.90$, Figure 1e) with oxygen exposure times as calculated by Koho et al. (2013) and Lengger et al. (2014). Similarly, organic carbon content in the core tops was negatively correlated with oxygen exposure times ($R^2 = 0.93$, from Lengger et al., 2014). The increase mirrors the decrease in % TOC – and thus progressing degradation – with increasing oxygen exposure time (Fig. 1b,c, Lengger et al., 2014). At P900, where the whole depth of the core was analysed, values increased slightly with depth, from -21.5 ‰ at the surface, to -20.9 ‰ (Fig. 3). $\delta^{13}C$ values of particulate organic carbon (suspended particulate organic matter) decreased throughout the water column from – 19 to – 21.8 ‰, though with a substantially ^{13}C-depleted, yet unexplained, value at the very surface (20 m depth) of – 22.9 ‰ (Fig. S1).
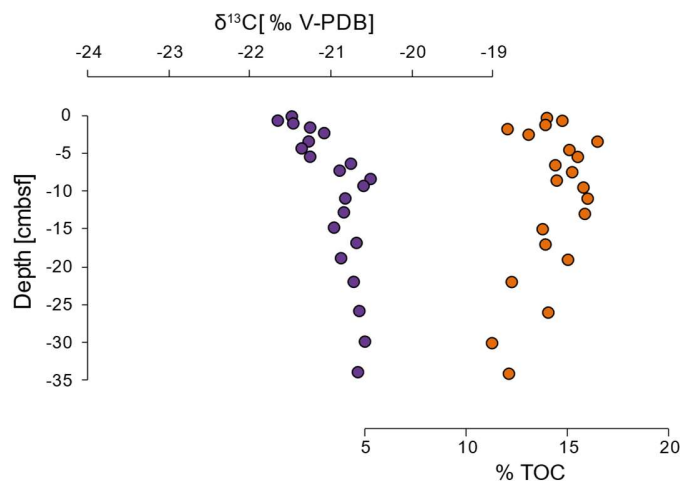
Figure 3. Depth profile of $\delta^{13}C_{org}$ and % TOC in an unamended core at P900.

3.2.   Biomarkers

3.2.1. Bacteriohopanepolyols (BHPs)

Analysis of BHPs in the Arabian Sea cores using both HPLC-APCI-MS and HTGC-MS, all showed that BHT', specific for *Scalindua*, was abundant, and the fractional abundance of BHT's when compared to the sum of BHT and BHT' ranged from 0.4 to 0.6. Other, relatively non-source-specific, BHPs were also present: BHT, 35-aminobacteriohopane-32,33,34-triol

294   (aminotriol), bacteriohopane-31,32,33,34,35-pentol (BHpentol), bacteriohopanetetrol cyclitol
295   ether (BHT-CE) and anhydro-BHT (Fig. S3). The relative concentrations of
296   bacteriohopanetetrols were 75 to 96 % of total bacteriohopanepolyols, an order of magnitude
297   higher than other BHPs (Fig. S3). HTGC-MS was able to detect BHT, BHT' and BHpentol (Fig.
298   S2), as well as small amounts of anhydroBHT, a BHT degradation product, and BHP-570, which
299   has been tentatively identified by Sessions et al. (2013) as acetylated bacteriohopanediol,
300   possibly also a degradation product of bacteriohopanetetrol. In the core from P900, the ratio of
301   BHT' over BHT increased with depth (Fig. S4).

302   We also analysed the BHP content of sediment cores incubated with ^{13}C-labelled organic
303   matter at both sites under the different conditions detailed by Pozzato et al. (2013 a, b), which
304   was respired and generated ^{13}C-labelled DIC, allowing to trace autotrophic processes such as
305   anammox. No changes were noted, except for in P900; in those, BHT abundance increased (i.e.
306   BHT'/BHT decreased), indicating that some of the sedimentary BHT could have been produced
307   in situ (Fig. S4).

308   3.2.2.   BHT and BHT' δ^{13}C values

309   To establish the isotopic difference of BHT and BHT' derived from anammox we
310   analysed biomass obtained from a batch reactor. BHT and BHT' were the main biohopanoids in
311   the biomass from '*Ca.* S. profunda' detected by HTGC-MS (Fig. S2b). In addition to being
312   present in '*Ca Scalindua sp.*' anammox bacteria, BHT is a ubiquitous lipid common to many
313   bacteria, BHT', however, is specific to *Ca Scalindua sp.*' in marine environments (Rush et al.,
314   2014). The δ^{13}C values of BHT and BHT' were identical within the error of analysis (-49 and -
315   48 ‰, respectively; Table 1), indicating identical fractionation and thus biosynthetic pathways
316   for both lipids.

317   In the Arabian Sea sediments (all unamended cores), BHT was markedly enriched in ^{13}C
318   relative to BHT', with values ranging from -24.7 to -28.8 ‰ and -39.1 to -48.1 ‰, respectively
319   (Figs. 4b-c). At P1800 (below the OMZ), BHT and BHT' were slightly more depleted in ^{13}C,
320   with BHT at -27 ± 3 ‰ and BHT' at -47 ± 4 ‰, as compared to -26 ± 1 ‰ and -43 ± 5 ‰ for
321   BHT and BHT' at P900 (in the OMZ). However, the difference between P900 and P1800 was
322   not statistically significant for either BHT or BHT'. Moreover, even though the proportion of
323   BHT' increased with depth in the anoxic core, the δ^{13}C values did not change. We also analysed
324   BHT and BHT' in the cores that had been incubated with ^{13}C-labeled POM and DOM, and these
325   showed no indication of ^{13}C-enrichment in BHT'. Excluding outliers (defined by a Grubbs test at
326   99% confidence level and indicated in Table 1), BHT' values were on average -48 ± 4 ‰ and -
327   46 ± 2 ‰ at P1800, and P900, respectively. BHT was slightly enriched compared to the
328   unamended incubations at 3 cm depth ($\Delta\delta^{13}$C = 4.6 ± 0.7 ‰), but not at 1 cm depth. BHpentol
329   concentrations were too low to allow reliable isotopic determination, and anhydroBHT and BHP-
330   570 co-eluted with other compounds, also precluding their isotopic characterization.

331   **4.   Discussion**

332   4.1.   Origins of BHT and BHT' - a biomarker for anammox

333   BHT', a biomarker likely unique for annamox in marine environments (Rush et al.,
334   2014,), is highly abundant in the sediment and occurred throughout both sediment cores (Fig.
335   4a), suggesting a significant contribution of anammox biomass to sedimentary organic matter. In

336 the anoxic core (P900), BHT and BHT' were present in concentrations at least an order of
337 magnitude higher than other BHPs (Fig. S2), and BHT' was the most abundant of the two
338 stereoisomers (Fig. 4a). The high fractional abundance of BHT' over the sum of BHT and BHT'
339 (0.4 – 0.6) is contrary to our expectations, as BHT is a ubiquitous lipid and presumed to derive
340 from both anammox and non-anammox sources such as cyano- and many other bacteria (Pearson
341 and Rusch, 2009); it is, therefore, expected to be abundant in most depositional contexts. Lower
342 proportions of BHT were reported previously in nearby core tops (0.22-0.30) by Saenz et al.
343 (2011); this could be caused by a difference in settings, or in BHP extraction protocol. However,
344 the high proportions of BHT' observed in the Arabian Sea are not unprecedented: they are
345 slightly lower than BHT' proportions in sediments underlying the Humboldt Current System
346 OMZ offshore Peru (0.45 – 0.69 in surface sediments, Matys et al., 2017).
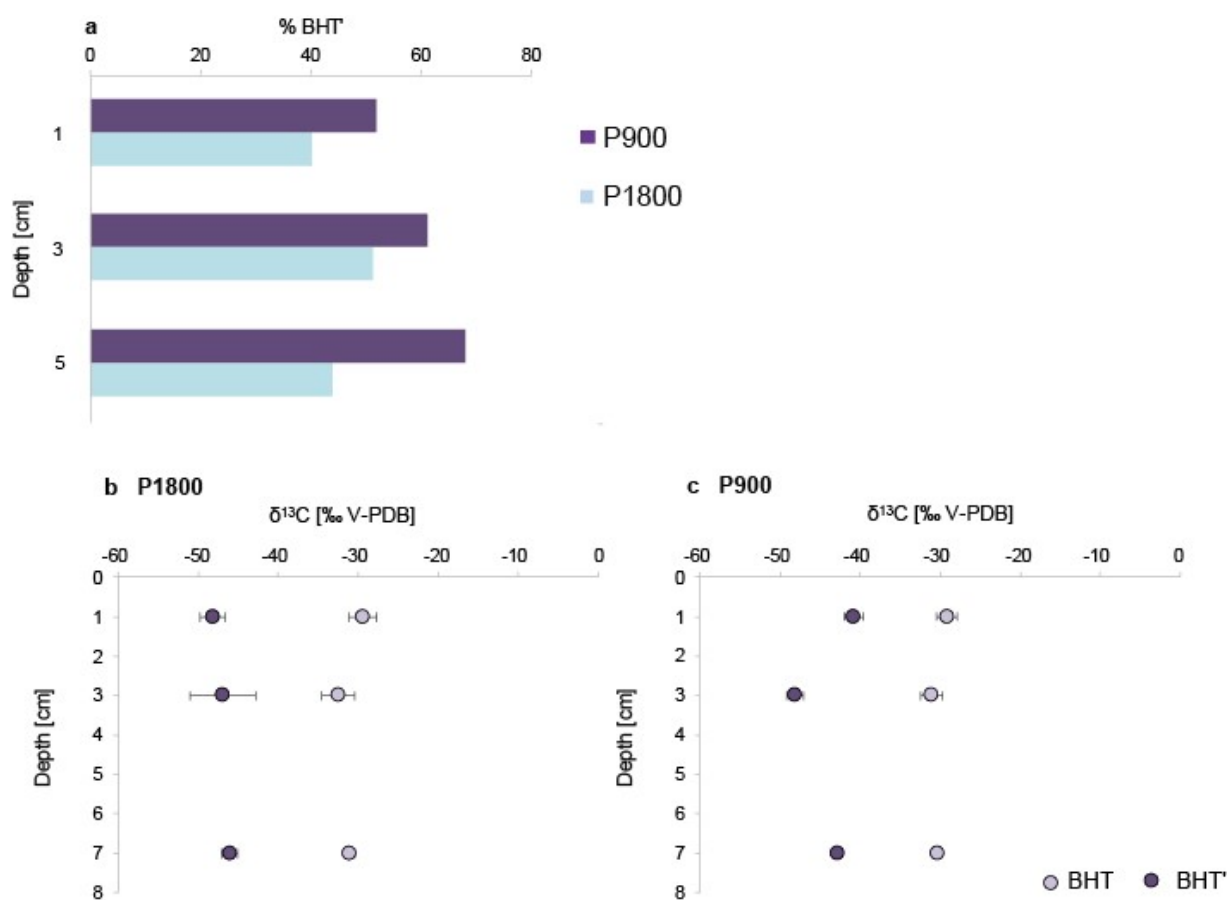
347
348
349 **Figure 4**. Anammox biomarkers in unamended Arabian Sea sediment. Panel (a) shows the
350 proportion of BHT' relative to BHT+BHT', panels (b) and (c) show the $\delta^{13}C$ values of BHT and
351 BHT' in the unamended oxic (P1800) and anoxic core (P900), respectively.

352

353 Supporting evidence for the unique source of BHT' comes from its ^{13}C values of -40 to -
354 50‰. Anammox bacteria are known to fractionate strongly against $\delta^{13}C$, with up to 26 ‰
355 fractionation observed for biomass in cultures and sediment, with even more strongly depleted
356 BHT and BHT' (Brocadia sp. by 47 ‰ and Scalindua sp. by 49 ‰ against DIC; Schouten et al.,
357 2004). Anammox bacteria within the oxygen minimum zone and using dissolved inorganic

358 carbon, which is up to 2 ‰ lighter within the OMZ than at the surface (Kroopnick, 1984), are
359 likely to produce such ^{13}C-depleted lipids. In line with an anammox origin, BHT' here is
360 decidedly more depleted than other biomarkers in the Arabian Sea (cf. Wakeham and McNichol,
361 2014), though distinctly depleted highly branched isoprenoids (HBIs, -37 ‰) have been found in
362 Arabian Sea cores from the Holocene (Schouten et al., 2000).

363 BHT, however, is much more enriched in ^{13}C in the Arabian Sea sediments, with values
364 of -29 to -30 ‰ (Fig. 4b,c). This is in contrast to anammox cultures, where BHT and BHT' are
365 produced with identical isotope values (Fig. S4, Table 1). This strongly supports the idea that
366 BHT has a mixed origin. The sources for BHT could be varied: cyanobacteria or heterotrophic
367 bacteria thriving in the OMZ or the sediment (Pearson and Rusch, 2009), and possibly including
368 nitrite-oxidising bacteria (Kharbush et al., 2018). The δ^{13}C values of BHT derived from these
369 alternative sources are poorly constrained (Hayes, 2001; Kharbush et al., 2018; Pearson, 2010;
370 Sakata et al., 1997; Schouten et al., 1998). However, for heterotrophic bacteria, values similar to
371 the consumed OM minus the depletion associated with polyisoprenoids of 6-8 ‰ are expected
372 (Pancost and Sinninghe Damsté, 2003). Similar values would be expected for cyanobacterial
373 lipids, too, as those are depleted by 22 – 30 ‰ compared to dissolved CO_2, which varies from 0
374 to 2 ‰ in the photic zone. Methane cycling could also lead to ^{13}C depleted OM, but is not
375 important in the Arabian Sea (Lüke et al., 2016), and there is no biomarker evidence for it, such
376 as ^{13}C depleted archaeal lipids, or methylated BHPs. Thus, a BHT δ^{13}C value of -30 ‰ suggests
377 heterotrophic and other bacterial sources, possibly mixed with an anammox source.

378 Anammox activity has been shown to occur both within the OMZ water column (Jensen
379 et al., 2011; Lüke et al., 2016; Pitcher et al., 2011; Villanueva et al., 2014) as well as in
380 sediments (Sokoll et al., 2012; Devol, 2015). To test whether the anammox-derived biomarkers
381 are formed in the sediment, the labelled cores were incubated for 7 days with particulate and
382 dissolved organic matter (Table 1), which resulted in the substantial incorporation of ^{13}C into
383 bacterial fatty acids, as well as generating ^{13}C-enriched CO_2 due to heterotrophic respiration (up
384 to 14 % of the added C was respired, Pozzato et al., 2013a,b). Anammox bacteria are
385 autotrophic, and it is therefore likely that an active sedimentary community would result in some
386 uptake of this ^{13}C labelled CO_2 formed by respiration. However, no significant labelling was
387 observed in BHT' or BHT (Table 1, Table S1), suggesting that most of this pool is water-column
388 derived. Further, BHT and BHT' are also present in the surface of the oxic sediments (P1800), in
389 proportions similar to the anoxic sediments at P900. Even if anammox growth was too slow for
390 labelling to take effect, substantial sedimentary production would have resulted in a decreasing
391 δ^{13}C value of BHT' in the unamended cores, as DIC gradually becomes more ^{13}C depleted with
392 sediment depth (Fernandes et al., 2018), but this is not observed (Fig. 4bc). Collectively, these
393 data support the idea that the vast majority of BHT' is derived from anammox bacteria living in
394 the OMZ of the water column, and that BHT also has a predominant pelagic origin with limited
395 sedimentary production.

396 The δ^{13}C values of geohopanoids (i.e. the geological degradation product of biohopanoids such
397 as BHT and BHT') can exhibit dramatic variability, and often pronounced depletion in terrestrial
398 (Pancost et al., 2007) and marine settings (Köster et al., 1998). These are commonly attributed to
399 aerobic methane oxidising bacteria, and thus regarded as evidence for a significant contribution
400 of methane oxidisers to sedimentary organic matter. However, our data show that hopanes of -35
401 to -50 ‰ could also indicate the presence of a significant amount of anammox bacteria in an
402 anoxic water column. Several factors could attenuate the anammox signal. The decrease of

403   biohopanoids in structural complexity upon degradation means that the anammox signal would
404   be diluted by mixing with aerobically and anaerobically produced hopanoids such as those of
405   *Geobacter* (Fischer et al., 2005; Härtner et al., 2005). Chemoautotrophs operating in euxinic
406   settings employ biochemical pathways resulting in ^{13}C-enriched biomass and lipids compared to
407   DIC (van Breugel et al., 2005b). However, in anoxic basins such as the Black Sea or anoxic
408   fjords, remineralization of organic matter also results in distinctly depleted $\delta^{13}C_{DIC}$ below the
409   chemocline (-12 ‰; Fry et al., 1991; Volkov, 2000). This may explain why, in some marine
410   anoxic settings where we might expect to see an anammox signature, the ^{13}C depletion of
411   hopanes parallels that of algal biomarkers (Sinninghe Damsté et al., 2008; van Breugel et al.,
412   2005a). Nonetheless, we suggest that potential anammox contributions to the sedimentary
413   hopanoid pool should be considered when interpreting their abundances, distributions and
414   isotopic compositions.

415   4.2.   Origin of sedimentary organic matter

416   The Murray Ridge represents an open ocean setting, and the selected coring sites were in
417   close proximity to each other, with no substantial terrigenous contribution (Koho et al., 2013;
418   Lengger et al., 2014, 2012b; Nierop et al., 2017; Fig. 1d). Despite this, $\delta^{13}C$ values of
419   sedimentary organic matter of a purely marine origin varied: The value at the shallowest location
420   (-21.5 ‰; P900), within the OMZ, was 2.5 ‰ more depleted than the estimated value for surface
421   water-derived OM -19.8 ‰ (Fontugne and Duplessy, 1986), and the $\delta^{13}C$ values of sedimentary
422   C_{org} increased with increasing oxygen bottom water concentrations / oxygen exposure time (Fig.
423   1e). These observations agree with earlier studies from this setting. Cowie et al. (2009, 1999)
424   detected similar trends in surficial sediments across different settings in the Arabian Sea, with
425   values of -21 ‰ within and -19 ‰ above and below the OMZ. Organic matter in sediment traps
426   collected in the north western Arabian Sea (i.e. sinking POC) had a $\delta^{13}C$ value of -22.4 ‰
427   (composite of the OMZ between 500 and 900 m depth). The corresponding sedimentary $\delta^{13}C_{org}$
428   value, from oxygenated bottom waters at 1445 m depth, was, however, more enriched (-20.8‰;
429   Wakeham and McNichol, 2014). Fernandes et al. (2018) detected similar, though less
430   pronounced, trends in sediments collected from the Pakistan margin. An increase in $\delta^{13}C$ with
431   enhanced degradation, i.e. ^{13}C-enriched sediments vs. depleted POM, was also observed in the
432   South China Sea (Liu et al., 2007), and in the Eastern Tropical North Pacific (Jeffrey et al.,
433   1983).

434   Despite its common occurrence in OMZ settings, this trend is unusual and, at present, not
435   explained: degradation of organic carbon in marine environments usually preferentially removes
436   isotopically heavy carbon (Hatch and Leventhal, 1997), causing a depletion in $\delta^{13}C$ with
437   increased degradation of the sediment. This can be due to the removal of the more labile marine
438   carbon, and subsequent relative enrichment of terrigenous organic material of a lower initial
439   reactivity and lower $\delta^{13}C$ values (Huguet et al., 2008; Middelburg et al., 1993). However,
440   progressive depletion also occurs in areas with purely marine input; this is due to preferential
441   loss of ^{13}C-enriched carbohydrates over the more ^{13}C-depleted lipids, and preferential
442   degradation of easily accessible material over biopolymers (Spiker and Hatcher, 1987), and
443   polymerization and elimination of functional groups (Galimov, 1988; Balabane et al., 1987).
444   Conversely, sulfurization, a process observed in euxinic settings appears to preferentially
445   preserve ^{13}C-enriched material such as carbohydrates (Van Kaam-Peters et al., 1998); however,
446   this process is not expected to occur here - the Arabian Sea is anoxic but not sulfidic (Ulloa et
447   al., 2012) and has not experienced euxinia for the past 120 ka (Schenau et al., 2002).

448 Nonetheless, in Arabian Sea sediment, $\delta^{13}C_{org}$ values increased by 1.8 ‰ with increasing oxygen
449 exposure time and thus increasing degradation; at the same time, organic carbon contents
450 decreased from 60 to 10 mg g dw^{-1}, indicating progressing remineralization (Fig. 1c, Lengger et
451 al., 2014). Cowie (2005) attributed this to the contribution of – potentially – organic matter from
452 the facultatively autotrophic, chemosynthetic sulfur-bacterium *Thioploca* sp., which has been
453 observed in the Arabian Sea (Schmaljohann et al., 2001). However, *Thioploca* sp. has only been
454 reported for shelf and upper slope sediments in the Arabian Sea (above and upper part of OMZ),
455 and it is unlikely that the sulfur-dependent *Thioploca* sp. could have caused this significant
456 depletion by chemoautotrophy, as sulfide concentrations are negligible within the OMZ (Kraal et
457 al., 2012), and there is no evidence for the production of severely ^{13}C-depleted biomass by
458 filamentous sulfur bacteria (Zhang et al., 2005). Further, the depletion is not only observed in
459 sediments, but also in particle fluxes (Wakeham and McNichol, 2014), which strongly suggests
460 the exclusion of sedimentary sources for ^{13}C-depleted organic matter. This is also supported by
461 the $\delta^{13}C_{org}$ values of the suspended particulate matter (Fig. S1), which becomes gradually more
462 depleted with depth.

463 An active nitrogen-cycle in the water column within the Arabian Sea OMZ is
464 undisputedly present, with heterotrophic denitrifying bacteria, nitrifying archaea, nitrite-
465 oxidising and anammox bacteria present in high abundances (Lüke et al., 2016; Villanueva et al.,
466 2014). The ^{13}C fractionation for the carbon fixation pathways employed by nitrifying archaea (3-
467 Hydroxypropionate/4-Hydroxybutyrate, 3-HP/4-HB) is similar to that of phytoplankton using
468 Rubisco (Könneke et al., 2012). The biomass of heterotrophic denitrifiers is close to the value of
469 the source organic matter (1 ‰ more enriched; Hayes, 2001), and the biochemical pathway
470 employed by nitrite oxidisers (reverse TCA cycle) produces ^{13}C-enriched biomass (Pearson,
471 2010). Anammox bacteria, however, are abundant and active in the Arabian Sea (Jensen et al.,
472 2011) and known to produce highly ^{13}C-depleted biomass by inorganic carbon fixation
473 (Schouten et al., 2004). Anammox bacteria, and other, yet undescribed chemoautotrophs, could
474 thus present a potential pathway for addition of ^{13}C-depleted organic matter to sinking organic
475 matter, a hypothesis we explore further below.

476 The water-column derived ^{13}C-depleted BHT', in combination with the unusual $\delta^{13}C_{org}$
477 trends, suggests that there may be a substantial contribution of ^{13}C depleted organic carbon,
478 produced by anammox bacteria, to the sedimentary organic matter. Based on BHT' δ^{13}C values
479 determined in this study, and the fractionation factor associated with anammox lipid biosynthesis
480 of 16 ‰ (lipid versus total biomass; Schouten et al., 2004), we can estimate a δ^{13}C value for
481 anammox biomass: of ca.-28.6 ± 6 ‰, which is similar to the expected value calculated from
482 $\varepsilon_{biomass-DIC}$ (22-26 ‰; Schouten et al., 2004) and the generally observed DIC value in the Arabian
483 Sea OMZ at depth, 0 ‰ (Moos, 2000). This is significantly depleted compared to phytoplankton
484 biomass in the Arabian Sea (-19.8 ‰, Fontugne and Duplessly, 1978), and would add depleted
485 organic carbon to the sinking POM.

486 We modelled the contribution of annamox biomass ($\chi_{anammox}$) to SOM using an
487 isotopic mass balance approach (using IsoError; Phillips et al., 2005), which employs uncertainty
488 propagation and error estimates and allows the determination of contributions of likely sources
489 of organic matter to the sediment. The end member value of -19.8 ± 0.5 ‰ was used for
490 phytoplankton-derived SOM (Fontugne and Duplessy, 1986; Ziegler et al., 2008). This value is
491 slightly lower than the -19 ‰ observed from the surface particulate carbon, but is representative
492 of sedimentary organic matter, as it accounts for the decreased δ^{13}C values of POM caused by

493   degradation of ^{13}C enriched compounds such as carbohydrates (Close, 2019; Ziegler et al.,
494   2008). More recent values for phytoplankton δ^{13}C are, to the best of our knowledge, not
495   available. Planktonic, sinking organic matter, and organic material produced by heterotrophs also
496   contribute to sedimentary OM. However, this OM value would likely be similar to the organic
497   matter assimilated (Blair et al., 1985; 2001). -28.6 ± 6 ‰ was used for anammox-derived organic
498   carbon, as derived from the δ^{13}C value of BHT' and $\varepsilon_{bm/lipid}$ of 16 ± 4 ‰ (Schouten et al., 2004;
499   Table 1; uncertainty represents combined standard deviations of $\delta^{13}C_{BHT'}$ and $\varepsilon_{lipid/bm}$). The δ^{13}C
500   value -21.5‰ of surface sediment C_{org} in the OMZ was used as the value of the mixture (Table
501   1):

502
503

$$\chi_{anammox} \cdot \delta^{13}C_{anammox} + \chi_{PP} \cdot \delta^{13}C_{PP} = \text{-21.5 ‰}$$

504   Eqn 1
505   The modelling, assuming the above end member contributions and their statistical uncertainties,
506   yields a proportion of anammox with a mean of approximately 17% (Fig. 5), and confirms that,
507   with 95% confidence, anammox contribution to the sedimentary organic matter is between 3 and
508   30% among the different cores. This suggests that some of the sedimentary organic matter
509   (SOM) present at P900 is anammox-derived. However, other chemoautotrophic bacteria also
510   present, or suspected to be present, in the Arabian Sea OMZ (e.g. ammonia-oxidizing archaea,
511   Pitcher et al., 2011) possess metabolisms which would lead to different δ^{13}C values, and could
512   therefore be diluting this signal (Hayes, 2001; Pearson, 2010). These results suggest that the
513   contribution of prokaryotic organic material produced in the OMZ to SOM is larger than
514   estimated in this simple, two-component mass balance. A three-source model resolving
515   heterotrophic bacteria or degraded OM, anammox bacteria and phytoplankton was solved with
516   SIAR (Parnell et al., 2010) and yielded similar results (not shown).

517
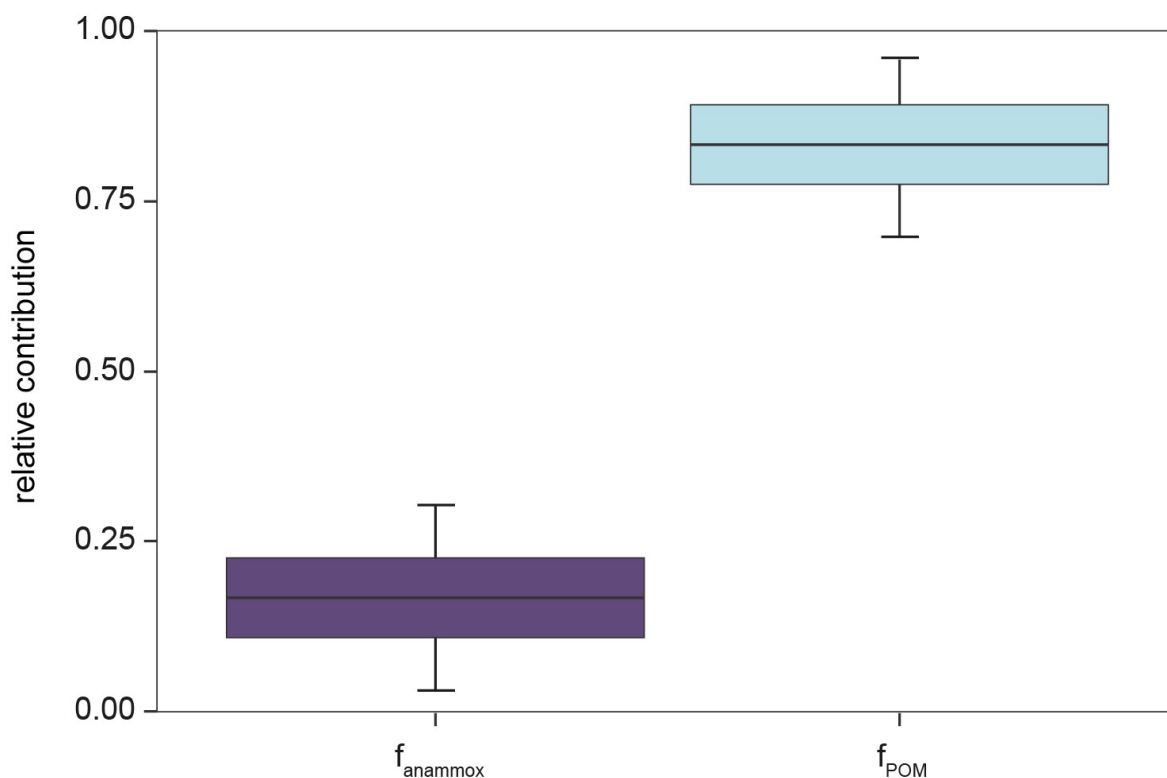
518 **Figure 5.** Results from the isotope mass balance model, showing the calculated means, standard
519 error, and confidence intervals for contribution from anammox, and planktonic-derived OM
520 (POM) to the surface sediment at P900.

521

522   This estimate, at a first glance, appears large. However, we can convert experimental
523 rates of anammox-mediated ammonia oxidation of $27 - 38$ nmol L^{-1} d^{-1} as determined in the
524 Arabian Sea (Jensen et al., 2011) and alternative rates of 0.24 -4.32 nmol L^{-1} d^{-1} estimated by
525 Ward et al. (2009), to carbon fixed using stoichiometric rates determined for anammox bacteria
526 of 0.07 mol C mol N_2^{-1} (Jetten et al., 2001; Strous et al., 1999; van de Vossenberg et al., 2008).
527 Assuming a production depth of 300 to 900 m water depth, with a maximum at 600 m (Pitcher et
528 al., 2011), anammox production over the whole depth could be estimated using Equation 2 (see
529 Fig. S5),

530

531
$$P = \frac{(k \cdot 600)}{2}$$

532   Eqn. 2
533 in which k corresponds to maximum rate at maximum production depth calculated from
534 aforementioned published anammox rates (k equals $138.7 - 9855$ µmol m^{-3} yr^{-1}, Jensen et al.
535 2011; $87.6 - 1576.8$ µmol m^{-3} yr^{-1}, Ward et al. 2009; Fig. S5).

536   Using this equation, we calculated that water-column anammox bacteria produce up to
537 3.5 g organic C m^{-2} yr^{-1}. These estimates dwarf sedimentary anammox rates, with C-fixation
538 determined to be at 64 pg organic C m^{-2} yr^{-1} in the Arabian Sea (Sokoll et al., 2012), indicating
539 that most of the anammox carbon in the sediment is water-column derived. Given organic carbon
540 accumulation rates (Lengger et al., 2012b) of 3 to 5 g C m^{-2} yr^{-1} at P900 and assuming a 17 %
541 anammox contribution to sedimentary organic matter, a maximum of 24 % of annually produced,
542 water-column anammox biomass is preserved in this anoxic setting. Within the sediment from
543 the OMZ, as seen from a sedimentary depth profile at P900 in the OMZ (Fig. 3), $\delta^{13}C_{org}$ also
544 shifts to higher values with depth, to a maximum of -20.8 ‰ at 8 cmbsf. However, contrary to
545 oxic degradation, no decrease in SOM contents occurs over the first 14 cm (Fig. 3). In this case,
546 the increase in $\delta^{13}C_{org}$ likely reflects input by other sedimentary autotrophs, producing enriched
547 organic carbon. This suggests that the ^{13}C-depleted SOM signal from the OMZ is not completely
548 preserved.

549   Other chemoautotrophs, where specific biomarkers are not available, could also
550 contribute to the SOM: at depth, the increased availability of CO_2 derived from heterotrophic
551 respiration of the POM pool would result in greater discrimination against ^{13}C (Freeman et al.,
552 1994; Freeman, 2001). An example are lipids of ammonia-oxidising archaea, which were more
553 depleted when deposited in the OMZ than below the OMZ (Table S2), suggesting that some of
554 those were produced in the produced in the OMZ and transported to the sediment (Lengger et al.,
555 2014, 2012b; Schouten et al., 2012).. However, as these archaeal lipids present a mixed pelagic
556 and sedimentary signal, quantitative estimates are not possible.

557   Hence, chemoautotrophic carbon fixation could explain the low δ^{13}C values of
558 sedimentary OM observed within the OMZ. As the newly produced organic carbon is more
559 labile than surface-produced organic matter, it would degrade more quickly upon exposure to

560   oxic bottom waters. This poorer preservation of anammox biomass results in a shift back towards
561   the ^{13}C signature of the primary photosynthetic production, which is observed as the enrichment
562   in sedimentary $\delta^{13}C_{org}$ with increasing oxygen exposure times (Fig. 1e). A likely explanation for
563   this lability of anammox biomass is that, due to the lack of zooplankton in the OMZ, this organic
564   matter is not fecal-pellet packaged or adsorbed to inorganic particles and thus not matrix
565   protected (cf. Burdige, 2007). Wakeham et al. (2002) analysed the biomarker fluxes in sinking
566   particles in the Arabian Sea, and they also found that surface-produced lipids such as alkenones
567   (which would be fecal pellet packaged) were exceptionally well-preserved compared to the total
568   organic carbon of the SPM. Gong and Hollander (1997) also noted an enhanced contribution of
569   bacterial biomass to sediment deposited under anoxic conditions in the Santa Monica Basin,
570   when compared to sediment located in nearby oxygenated bottom waters. Studies examining
571   carbon fluxes in the Arabian Sea (Keil et al., 2016) and the Cariaco basin (Taylor et al., 2001)
572   invoked the addition of chemoautotrophically derived carbon from a midwater source in order to
573   explain the enhanced carbon fluxes observed, even if oxygen depletion and other factors such as
574   the lack of zooplankton were taken into account.

575

576   ## 4.3.   Quantifying the biological pump and remineralization rates

577   Models of the biological pump consider primary production, particle fluxes, oxygen
578   concentrations, and respiratory rates. Sinking organic matter is traditionally regarded as a
579   reflection of exported organic material from the photic zone, and export models consider
580   remineralization and C-loss (Cabré et al., 2015; Schlitzer, 2002), based on claims that bacterial
581   contributions do not sink (Buesseler et al., 2007). However, relying on these parameters,
582   estimates of particulate organic carbon flux in the Arabian Sea are generally too low to sustain
583   experimentally observed denitrification, bacterial production, and oxygen deficiency in the
584   Arabian Sea (Anderson and Ryabchenko, 2009; Andrews et al., 2017; Naqvi and Shailaja, 1993;
585   Rixen and Ittekkot, 2005). New mechanisms have been discovered that can explain downward
586   transport of smaller particles and bacteria, such as particle aggregation (Burd and Jackson, 2009),
587   and mixed layer transport mechanisms (Bol et al., 2018), which enable the consideration of the
588   contribution of anammox biomass to sinking OM.

589   In previous work, the deficit in modelled and observed C-utilization estimated from
590   denitrification was as high as 70 g C m^{-2} y^{-1} (Naqvi and Shailaja, 1993). Including anammox in
591   models of the nitrogen cycle can account for at least 30% or more of the nitrogen losses, as well
592   as accounting for organic carbon production, thereby reconciling some of this budget
593   discrepancy. More recently, the combined inclusion of mesopelagic zooplankton and
594   heterotrophic bacteria into 3D models resulted in much lower bacterial productivity (4.7 g C m^{-2}
595   y^{-1}) than observational estimates of 10.4 g C m^{-2}y^{-1} (Anderson and Ryabchenko, 2009). Other
596   recent models, combined with experimental observations of particle fluxes, suggest that at some
597   stations, the lower oxycline is associated with 0.4 to 1.8 g C m^{-2} y^{-1} increases in net carbon fluxes
598   (Roullier et al., 2014). Horizontal transport, also from nepheloid layers, novel transport
599   mechanisms from the mixed layer, and DOM, have previously been invoked as the missing
600   carbon supply. Here, we estimate that an additional 3.5 g m^{-2} y^{-1} of organic carbon are produced
601   by anammox from DIC, with other chemoautotrophic processes possibly adding to this estimate.
602   This also affects estimates of nitrogen losses and has direct implications for the forecasting of
603   OMZs in a warming world.

604   In paleoceanography, the $\delta^{13}C$ values of total organic carbon are commonly used in
605 combination with organic carbon contents in sediment cores to interpret changes in sea surface
606 biogeochemistry and to discern the causes for ocean deoxygenation (Jenkyns, 2010; Meyers,
607 2014). Negative $\delta^{13}C$ excursions are associated with either atmospheric injection of depleted CO_2
608 and/or increased CO_2 availability (Pagani, 2005; Pancost and Pagani, 2005), or a higher input of
609 terrigenous organic matter. Positive excursions are inferred to reflect increased burial rates of
610 organic carbon, i.e. the removal of 'light' carbon from the ocean-atmosphere reservoir (e.g.
611 Kuypers et al., 2002; Jenkyns, 1985). An increase in TOC coinciding with a negative carbon
612 isotope excursion has been observed in the sedimentary record numerous times. They are a
613 prominent feature in OAE 1a (Leckie et al., 2002), during the PETM (Zachos et al., 2005), and in
614 the Eastern Mediterranean during Sapropel deposition (Meyers and Arnaboldi, 2008). Our results
615 show that if non-sulfidic OMZs expand to impinge on the sediment, a significant amount of ^{13}C-
616 depleted organic carbon can be preserved, changing the carbon isotope composition of organic
617 matter by up to – 1.6 ‰ in the case of Arabian Sea surface sediments, and by -0.5 to -1 ‰ in
618 deeper sediments. When evaluating past events based on bulk $\delta^{13}C$ values, the incorporation of
619 chemoautotrophically produced carbon must thus be considered. This also further supports
620 claims that calculations of pCO_2 based on differences between $\delta^{13}C$ of organic and inorganic
621 carbon should not rely on bulk organic carbon that includes bacterial contributions, but instead
622 use compound specific $\delta^{13}C$ values derived from algae, consistent with previous investigations
623 (Pancost et al., 1999; Pancost et al., 2013; reviewed by Witkowski et al., 2018). By extension, a
624 deviation from the relationship between $\delta^{13}C$ bulk OM and $\delta^{13}C$ phytane could be an indicator
625 for the chemoautotrophic contribution to sedimentary OM.

626   Chemoautotrophic metabolism in euxinic water columns, where often very low $\delta^{13}C_{DIC}$
627 values are observed (van Breugel et al., 2005a,b; Fry et al., 1991; Volkov, 2000), has previously
628 been invoked as contributing to organic matter in these setting. Anammox, which has been
629 shown to be an important process in the anoxic water column overlying euxinia (Kuypers et al.,
630 2003), also needs to be considered. Anammox also plays an important role in the nitrogen cycle
631 of Mediterranean sapropel events, even in sapropels where euxinia appears to have occurred
632 (Rush et al., 2019), potentially causing a significant contribution of anammox to the depleted
633 $\delta^{13}C_{org}$ values of these sapropels. Previously, a conceptual model invoking chemoautotrophy has
634 been invoked to explain e.g. the End-Permian (Luo et al., 2014) and the Lomagundi isotope
635 excursion (Bekker et al., 2008).

636   Settings similar to the Arabian Sea, with ≤ 4.5 μmol kg^{-1} O_2, occur in the East Pacific and
637 those settings in total occupy an area of 8.45 to 15 x 10^{12} m^2 (Karstensen et al., 2008; Hattori,
638 1983; Paulmier and Ruiz-Pino, 2009), or a volume of 0.46 x 10^{15} m^3 with 1.148 x 10^{12} m^2 in
639 contact with the sediment (Helly and Levin, 2004). OMZs are expanding in size and in volume
640 (Stramma et al., 2010; Queste et al., 2018), and anammox bacteria play a key role in these
641 settings, particularly because they tolerate higher oxygen concentrations than denitrifiers
642 (Dalsgaard et al., 2014). The labile organic matter added to the sinking carbon can fuel
643 heterotrophic processes, further exacerbating oxygen depletion, and nitrogen loss by
644 denitrification. For accurate future forecasting, it is imperative to reconcile experimental and
645 model-based estimates. Novel, detailed observations explaining the vertical transport of bacterial
646 biomass, and evidence from the isotopic composition of TOC and biomarkers for
647 chemoautotrophic processes, such as shown here for anammox, will enable the further
648 unravelling of the biogeochemical mechanisms underpinning present, past, and future OMZs.

5 Conclusions

Combining the $\delta^{13}C$ values of BHT', a biomarker from anammox bacteria, and the $\delta^{13}C$ values of sedimentary organic matter allowed us to estimate the contribution of anammox to SOM in the Arabian Sea. This can be as much as 30 % of organic matter deposited within the OMZ. In the sediments underlying the Arabian Sea, $\delta^{13}C$ values of total organic matter can shift by 1 to 2 ‰ due to these bacterial contributions, but it remains unclear how well and under what conditions this signature is preserved. Our results suggest that chemoautotrophs (e.g. anammox bacteria) contribute more than previously believed to the burial of carbon in oxygen deficient zones, and remineralization rates are potentially higher than inferred from organic matter decreases. This implies that, when past occurrences of OMZs are evaluated based on $\delta^{13}C$ values of SOM, a ^{13}C-depleted contribution of bacteria needs to be considered. Chemoautotrophic carbon fixation thus represents a mechanism of CO_2 removal from the pelagic water column, and contributes to fluxes of sinking organic carbon. It explains some of the mismatches in carbon budgets when experimental and modelling estimates are compared - and it should therefore be included in biogeochemical models predicting feedbacks to a warming world.

Data statement: Data statement: All supporting data is included, and will be deposited on Pangaea as appropriate.

683

References

Anderson, T. R., & Ryabchenko, V. A. (2009). Carbon cycling in the Mesopelagic Zone of the central Arabian Sea: Results from a simple model. *Washington DC American Geophysical Union Geophysical Monograph Series, 185*, 281–297. https://doi.org/10.1029/2007GM000686

Andrews, O., Buitenhuis, E., Le Quéré, C., & Suntharalingam, P. (2017). Biogeochemical modelling of dissolved oxygen in a changing ocean. *Philosophical Transactions of the Royal Society A: Mathematical, Physical and Engineering Sciences*, *375*(2102), 20160328. https://doi.org/10.1098/rsta.2016.0328

Angelis, Y. S., Kioussi, M. K., Kiousi, P., Brenna, J. T., & Georgakopoulos, C. G. (2012). Examination of the kinetic isotopic effect to the acetylation derivatization for the gas chromatographic-combustion-isotope ratio mass spectrometric doping control analysis of endogenous steroids: Kinetic isotopic effect to the acetylation derivatization of endogenous steroids. *Drug Testing and Analysis*, *4*(12), 923–927. https://doi.org/10.1002/dta.408

Balabane, M., Galimov, E., Hermann, M., & Létolle, R. (1987). Hydrogen and carbon isotope fractionation during experimental production of bacterial methane. *Organic Geochemistry*, *11*(2), 115–119. https://doi.org/10.1016/0146-6380(87)90033-7

Bekker, A., Holmden, C., Beukes, N. J., Kenig, F., Eglinton, B., & Patterson, W. P. (2008). Fractionation between inorganic and organic carbon during the Lomagundi (2.22–2.1 Ga) carbon isotope excursion. *Earth and Planetary Science Letters*, *271*(1), 278–291. https://doi.org/10.1016/j.epsl.2008.04.021

Blair, N., Leu, A., Muñoz, E., Olsen, J., Kwong, E., & Marais, D. D. (1985). Carbon isotopic fractionation in heterotrophic microbial metabolism. *Applied and Environmental Microbiology*, *50*(4), 996–1001.

Bol, R., Henson, S. A., Rumyantseva, A., & Briggs, N. (2018). High-Frequency Variability of Small-Particle Carbon Export Flux in the Northeast Atlantic. *Global Biogeochemical Cycles, 32*(12), 1803–1814. https://doi.org/10.1029/2018GB005963

Breitburg, D., Levin, L. A., Oschlies, A., Grégoire, M., Chavez, F. P., Conley, D. J., et al. (2018). Declining oxygen in the global ocean and coastal waters. *Science*, *359*(6371), eaam7240. https://doi.org/10.1126/science.aam7240

van Breugel, Y., Schouten, S., Paetzel, M., Nordeide, R., & Sinninghe Damsté, J. S. (2005a). The impact of recycling of organic carbon on the stable carbon isotopic composition of dissolved inorganic carbon in a stratified marine system (Kyllaren fjord, Norway). *Organic Geochemistry*, *36*(8), 1163–1173. https://doi.org/10.1016/j.orggeochem.2005.03.003

van Breugel, Y., Schouten, S., Paetzel, M., Ossebaar, J., & Sinninghe Damsté, J. S. (2005b). Reconstruction of $\delta^{13}C$ of chemocline CO^2 (aq) in past oceans and lakes using the $\delta^{13}C$ of fossil isorenieratene. *Earth and Planetary Science Letters*, 235(1), 421–434. https://doi.org/10.1016/j.epsl.2005.04.017

Buesseler, K. O., Antia, A. N., Chen, M., Fowler, S. W., Gardner, W. D., Gustafsson, O., et al. (2007). An assessment of the use of sediment traps for estimating upper ocean particle fluxes. *Journal of Marine Research, 65*(3), 345–416. https://doi.org/10.1357/002224007781567621

Burd, A. B., & Jackson, G. A. (2009). Particle Aggregation. *Annual Review of Marine Science, 1*(1), 65–90. https://doi.org/10.1146/annurev.marine.010908.163904 Burdige, D. J. (2007). Preservation of Organic Matter in Marine Sediments: Controls, Mechanisms, and an Imbalance in Sediment Organic Carbon Budgets? *Chemical Reviews*, *107*(2), 467–485. https://doi.org/10.1021/cr050347q

Cabré, A., Marinov, I., Bernardello, R., & Bianchi, D. (2015). Oxygen minimum zones in the tropical Pacific across CMIP5 models: mean state differences and climate change trends. *Biogeosciences*, *12*(18), 5429–5454. https://doi.org/10.5194/bg-12-5429-2015

Canfield, D. E. (2006). Models of oxic respiration, denitrification and sulfate reduction in zones of coastal upwelling. *Geochimica et Cosmochimica Acta*, *70*(23), 5753–5765. https://doi.org/10.1016/j.gca.2006.07.023

Close, H. G. (2019). Compound-Specific Isotope Geochemistry in the Ocean. *Annual Review of Marine Science*, *11*(1), 27–56. https://doi.org/10.1146/annurev-marine-121916-063634

Cooke, M. P., Talbot, H. M., & Farrimond, P. (2008). Bacterial populations recorded in bacteriohopanepolyol distributions in soils from Northern England. *Organic Geochemistry*, *39*(9), 1347–1358. https://doi.org/10.1016/j.orggeochem.2008.05.003

Cooke, M. P., van Dongen, B. E., Talbot, H. M., Semiletov, I., Shakhova, N., Guo, L., & Gustafsson, Ö. (2009). Bacteriohopanepolyol biomarker composition of organic matter exported to the Arctic Ocean by seven of the major Arctic rivers. *Organic Geochemistry, 40*(11), 1151–1159. https://doi.org/10.1016/j.orggeochem.2009.07.014

Cowie, G. (2005). The biogeochemistry of Arabian Sea surficial sediments: A review of recent studies. *Progress in Oceanography*, *65*(2), 260–289. https://doi.org/10.1016/j.pocean.2005.03.003

Cowie, G. L., & Hedges, J. I. (1992). Sources and reactivities of amino acids in a coastal marine environment. *Limnology and Oceanography*, *37*(4), 703–724. https://doi.org/10.4319/lo.1992.37.4.0703

Cowie, G. L., Calvert, S. E., Pedersen, T. F., Schulz, H., & von Rad, U. (1999). Organic content and preservational controls in surficial shelf and slope sediments from the Arabian Sea (Pakistan margin). *Marine Geology*, *161*(1), 23–38. https://doi.org/10.1016/S0025-3227(99)00053-5

753 Cowie, G. L., Mowbray, S., Lewis, M., Matheson, H., & McKenzie, R. (2009). Carbon and
754 nitrogen elemental and stable isotopic compositions of surficial sediments from the Pakistan
755 margin of the Arabian Sea. *Deep Sea Research Part II: Topical Studies in Oceanography*, *56*(6),
756 271–282. https://doi.org/10.1016/j.dsr2.2008.05.031

757 Dalsgaard, T., Stewart, F. J., Thamdrup, B., Brabandere, L. D., Revsbech, N. P., Ulloa, O., et al.
758 (2014). Oxygen at Nanomolar Levels Reversibly Suppresses Process Rates and Gene Expression
759 in Anammox and Denitrification in the Oxygen Minimum Zone off Northern Chile. *MBio, 5*(6),
760 e01966-14. https://doi.org/10.1128/mBio.01966-14

761 Devol, A. H. (2015). Denitrification, Anammox, and N_2 Production in Marine Sediments.
762 *Annual Review of Marine Science, 7*(1), 403–423. https://doi.org/10.1146/annurev-marine-
763 010213-135040

764 Dunne, J. P., Sarmiento, J. L., & Gnanadesikan, A. (2007). A synthesis of global particle export
765 from the surface ocean and cycling through the ocean interior and on the seafloor. *Global
766 Biogeochemical Cycles*, *21*(4). https://doi.org/10.1029/2006GB002907

767 Fernandes, S., Mazumdar, A., Bhattacharya, S., Peketi, A., Mapder, T., Roy, R., et al. (2018).
768 Enhanced carbon-sulfur cycling in the sediments of Arabian Sea oxygen minimum zone center.
769 *Scientific Reports*, *8*(1), 8665. https://doi.org/10.1038/s41598-018-27002-2

770 Fischer, W. W., Summons, R. E., & Pearson, A. (2005). Targeted genomic detection of
771 biosynthetic pathways: anaerobic production of hopanoid biomarkers by a common sedimentary
772 microbe. *Geobiology*, *3*(1), 33–40. https://doi.org/10.1111/j.1472-4669.2005.00041.x

773 Fontugne, M., & Duplessy, J. C. (1978). Carbon isotope ratio of marine plankton related to
774 surface water masses. *Earth and Planetary Science Letters*, *41*(3), 365–371.
775 https://doi.org/10.1016/0012-821X(78)90191-7

776 Fontugne, M. R., & Duplessy, J.-C. (1986). Variations of the monsoon regime during the upper
777 quaternary: Evidence from carbon isotopic record of organic matter in North Indian Ocean
778 sediment cores. *Palaeogeography, Palaeoclimatology, Palaeoecology*, *56*(1), 69–88.
779 https://doi.org/10.1016/0031-0182(86)90108-2

780 Freeman, K. H. (2001). Isotopic Biogeochemistry of Marine Organic Carbon. *Reviews in
781 Mineralogy and Geochemistry, 43*(1), 579–605. https://doi.org/10.2138/gsrmg.43.1.579

782 Freeman, K. H., Wakeham, S. G., & Hayes, J. M. (1994). Predictive isotopic biogeochemistry:
783 Hydrocarbons from anoxic marine basins. *Organic Geochemistry*, *21*(6), 629–644.
784 https://doi.org/10.1016/0146-6380(94)90009-4

785 Fry, B., Jannasch, H. W., Molyneaux, S. J., Wirsen, C. O., Muramoto, J. A., & King, S. (1991).
786 Stable isotope studies of the carbon, nitrogen and sulfur cycles in the Black Sea and the Cariaco
787 Trench. *Deep Sea Research Part A. Oceanographic Research Papers, 38*, S1003–S1019.
788 https://doi.org/10.1016/S0198-0149(10)80021-4

789 Galimov, E. M. (1988). Sources and mechanisms of formation of gaseous hydrocarbons in
790 sedimentary rocks. *Chemical Geology*, *71*(1), 77–95. https://doi.org/10.1016/0009-
791 2541(88)90107-6

792 Gong, C., & Hollander, D. J. (1997). Differential contribution of bacteria to sedimentary organic
793 matter in oxic and anoxic environments, Santa Monica Basin, California. *Organic Geochemistry*,
794 *26*(9), 545–563. https://doi.org/10.1016/S0146-6380(97)00018-1

795 Härtner, T., Straub, K. L., & Kannenberg, E. (2005). Occurrence of hopanoid lipids in anaerobic
796 Geobacter species. *FEMS Microbiology Letters*, *243*(1), 59–64.
797 https://doi.org/10.1016/j.femsle.2004.11.039

798 Hartnett, H. E., Keil, R. G., Hedges, J. I., & Devol, A. H. (1998). Influence of oxygen exposure
799 time on organic carbon preservation in continental margin sediments. *Nature*, *391*(6667), 572–
800 575. https://doi.org/10.1038/35351

801 Hatch, J. R., & Leventhal, J. S. (1997). Early diagenetic partial oxidation of organic matter and
802 sulfides in the Middle Pennsylvanian (Desmoinesian) Excello Shale member of the Fort Scott
803 Limestone and equivalents, northern Midcontinent region, USA. *Chemical Geology*, *134*(4),
804 215–235. https://doi.org/10.1016/S0009-2541(96)00006-X

805 Hayes, J. M. (2001). Fractionation of Carbon and Hydrogen Isotopes in Biosynthetic Processes.
806 *Reviews in Mineralogy and Geochemistry*, *43*(1), 225–277.
807 https://doi.org/10.2138/gsrmg.43.1.225

808 Hedges, J. I., & Keil, R. G. (1995). Sedimentary organic matter preservation: an assessment and
809 speculative synthesis. *Marine Chemistry*, *49*(2), 81–115. https://doi.org/10.1016/0304-
810 4203(95)00008-F

811 Helly, J. J., & Levin, L. A. (2004). Global distribution of naturally occurring marine hypoxia on
812 continental margins. *Deep Sea Research Part I: Oceanographic Research Papers, 51*(9), 1159–
813 1168. https://doi.org/10.1016/j.dsr.2004.03.009Herndl, G. J., & Reinthaler, T. (2013). Microbial
814 control of the dark end of the biological pump. *Nature Geoscience*, *6*(9), 718–724.
815 https://doi.org/10.1038/ngeo1921

816 Hollander, D. J., & Smith, M. A. (2001). Microbially mediated carbon cycling as a control on the
817 $\delta^{13}C$ of sedimentary carbon in eutrophic Lake Mendota (USA): new models for interpreting
818 isotopic excursions in the sedimentary record. *Geochimica et Cosmochimica Acta*, *65*(23), 4321–
819 4337. https://doi.org/10.1016/S0016-7037(00)00506-8

820 Huguet, C., de Lange, G. J., Gustafsson, Ö., Middelburg, J. J., Sinninghe Damsté, J. S., &
821 Schouten, S. (2008). Selective preservation of soil organic matter in oxidized marine sediments
822 (Madeira Abyssal Plain). *Geochimica et Cosmochimica Acta*, *72*(24), 6061–6068.
823 https://doi.org/10.1016/j.gca.2008.09.021

824   Jaeschke, A., Ziegler, M., Hopmans, E. C., Reichart, G.-J., Lourens, L. J., Schouten, S., &
825   Sinninghe Damsté, J. S. (2009). Molecular fossil evidence for anaerobic ammonium oxidation in
826   the Arabian Sea over the last glacial cycle: Anammox in the Arabian Sea. *Paleoceanography*,
827   *24*(2), n/a-n/a. https://doi.org/10.1029/2008PA001712

828   Jeffrey, A. W. A., Pflaum, R. C., Brooks, J. M., & Sackett, W. M. (1983). Vertical trends in
829   particulate organic carbon ^{13}C: ^{12}C ratios in the upper water column. *Deep Sea Research Part A.*
830   *Oceanographic Research Papers*, *30*(9), 971–983. https://doi.org/10.1016/0198-0149(83)90052-
831   3

832   Jenkyns, H. C. (1985). The early Toarcian and Cenomanian-Turonian anoxic events in Europe:
833   comparisons and contrasts. *Geologische Rundschau, 74*(3), 505–518.
834   https://doi.org/10.1007/BF01821208

835   Jenkyns, H. C. (2010). Geochemistry of oceanic anoxic events: REVIEW. *Geochemistry,*
836   *Geophysics, Geosystems*, *11*(3). https://doi.org/10.1029/2009GC002788

837   Jensen, M. M., Lam, P., Revsbech, N. P., Nagel, B., Gaye, B., Jetten, M. S., & Kuypers, M. M.
838   (2011). Intensive nitrogen loss over the Omani Shelf due to anammox coupled with dissimilatory
839   nitrite reduction to ammonium. *The ISME Journal*, *5*(10), 1660–1670.
840   https://doi.org/10.1038/ismej.2011.44

841   Jetten, M. S. M., Wagner, M., Fuerst, J., van Loosdrecht, M., Kuenen, G., & Strous, M. (2001).
842   Microbiology and application of the anaerobic ammonium oxidation ('anammox') process.
843   *Current Opinion in Biotechnology*, *12*(3), 283–288. https://doi.org/10.1016/S0958-
844   1669(00)00211-1

845   Keil, R. G., Neibauer, J. A., Biladeau, C., van der Elst, K., & Devol, A. H. (2016). A multiproxy
846   approach to understanding the "enhanced" flux of organic matter through the oxygen-deficient
847   waters of the Arabian Sea. *Biogeosciences*, *13*(7), 2077–2092. https://doi.org/10.5194/bg-13-
848   2077-2016

849   Keil, Richard G., Montluçon, D. B., Prahl, F. G., & Hedges, J. I. (1994). Sorptive preservation of
850   labile organic matter in marine sediments. *Nature*, *370*(6490), 549–552.
851   https://doi.org/10.1038/370549a0

852   Kharbush, J. J., Thompson, L. R., Haroon, M. F., Knight, R., & Aluwihare, L. I. (2018).
853   Hopanoid-producing bacteria in the Red Sea include the major marine nitrite oxidizers. *FEMS*
854   *Microbiology Ecology*, *94*(6). https://doi.org/10.1093/femsec/fiy063

855   Koho, K. A., Nierop, K. G. J., Moodley, L., Middelburg, J. J., Pozzato, L., Soetaert, K., et al.
856   (2013). Microbial bioavailability regulates organic matter preservation in marine sediments.
857   *Biogeosciences*, *10*(2), 1131–1141. https://doi.org/10.5194/bg-10-1131-2013

858 Könneke, M., Lipp, J. S., & Hinrichs, K.-U. (2012). Carbon isotope fractionation by the marine
859 ammonia-oxidizing archaeon Nitrosopumilus maritimus. *Organic Geochemistry*, *48*, 21–24.
860 https://doi.org/10.1016/j.orggeochem.2012.04.007

861 Köster, J., Rospondek, M., Schouten, S., Kotarba, M., Zubrzycki, A., & Sinninghe Damste, J. S.
862 (1998). Biomarker geochemistry of a foreland basin: the Oligocene Menilite Formation in the
863 Flysch Carpathians of Southeast Poland. *Organic Geochemistry*, *29*(1), 649–669.
864 https://doi.org/10.1016/S0146-6380(98)00182-X
865
866 Kroopnick, P. M. (1985). The distribution of ^{13}C of ΣCO_2 in the world oceans. *Deep Sea*
867 *Research Part A. Oceanographic Research Papers*, 32(1), 57–84. https://doi.org/10.1016/0198-
868 0149(85)90017-2

869 Kuypers, M. M. M., Sliekers, A. O., Lavik, G., Schmid, M., Jørgensen, B. B., Kuenen, J. G., et
870 al. (2003). Anaerobic ammonium oxidation by anammox bacteria in the Black Sea. *Nature*,
871 *422*(6932), 608–611. https://doi.org/10.1038/nature01472

872 Kuypers, Marcel M. M., Pancost, Richard D., Nijenhuis, Ivar A., & Sinninghe Damsté, Jaap S.
873 (2002). Enhanced productivity led to increased organic carbon burial in the euxinic North
874 Atlantic basin during the late Cenomanian oceanic anoxic event. *Paleoceanography*, *17*(4), 3–1.
875 https://doi.org/10.1029/2000PA000569

876 Lam, P., Lavik, G., Jensen, M. M., van de Vossenberg, J., Schmid, M., Woebken, D., et al.
877 (2009). Revising the nitrogen cycle in the Peruvian oxygen minimum zone. *Proceedings of the*
878 *National Academy of Sciences*, *106*(12), 4752–4757. https://doi.org/10.1073/pnas.0812444106

879 Lam, Phyllis, & Kuypers, M. M. M. (2010). Microbial Nitrogen Cycling Processes in Oxygen
880 Minimum Zones. *Annual Review of Marine Science*, *3*(1), 317–345.
881 https://doi.org/10.1146/annurev-marine-120709-142814

882 Lam, Phyllis, Jensen, M. M., Lavik, G., McGinnis, D. F., Müller, B., Schubert, C. J., et al.
883 (2007). Linking crenarchaeal and bacterial nitrification to anammox in the Black Sea.
884 *Proceedings of the National Academy of Sciences*, *104*(17), 7104–7109.
885 https://doi.org/10.1073/pnas.0611081104

886 Leckie, R. M., Bralower, T. J., & Cashman, R. (2002). Oceanic anoxic events and plankton
887 evolution: Biotic response to tectonic forcing during the mid-Cretaceous. *Paleoceanography*,
888 *17*(3), 13-1-13–29. https://doi.org/10.1029/2001PA000623

889 Lengger, S. K., Hopmans, E. C., Sinninghe Damsté, J. S., & Schouten, S. (2012a). Comparison
890 of extraction and work up techniques for analysis of core and intact polar tetraether lipids from
891 sedimentary environments. *Organic Geochemistry*, *47*, 34–40.
892 https://doi.org/10.1016/j.orggeochem.2012.02.009

893 Lengger, S. K., Hopmans, E. C., Reichart, G.-J., Nierop, K. G. J., Sinninghe Damsté, J. S., &
894 Schouten, S. (2012b). Intact polar and core glycerol dibiphytanyl glycerol tetraether lipids in the

895   Arabian Sea oxygen minimum zone. Part II: Selective preservation and degradation in sediments
896   and consequences for the TEX_{86}. *Geochimica et Cosmochimica Acta*, *98*, 244–258.
897   https://doi.org/10.1016/j.gca.2012.05.003

898   Lengger, S. K., Hopmans, E. C., Sinninghe Damsté, J. S., & Schouten, S. (2014). Impact of
899   sedimentary degradation and deep water column production on GDGT abundance and
900   distribution in surface sediments in the Arabian Sea: Implications for the TEX_{86}
901   paleothermometer. *Geochimica et Cosmochimica Acta*, *142*, 386–399.
902   https://doi.org/10.1016/j.gca.2014.07.013

903   Lengger, S. K., Sutton, P. A., Rowland, S. J., Hurley, S. J., Pearson, A., Naafs, B. D. A., et al.
904   (2018). Archaeal and bacterial glycerol dialkyl glycerol tetraether (GDGT) lipids in
905   environmental samples by high temperature-gas chromatography with flame ionization and time-
906   of-flight mass spectrometry detection. *Organic Geochemistry*, *121*, 10–21.
907   https://doi.org/10.1016/j.orggeochem.2018.03.012

908   Liu, K.-K., Kao, S.-J., Hu, H.-C., Chou, W.-C., Hung, G.-W., & Tseng, C.-M. (2007). Carbon
909   isotopic composition of suspended and sinking particulate organic matter in the northern South
910   China Sea—From production to deposition. *Deep Sea Research Part II: Topical Studies in
911   Oceanography*, *54*(14), 1504–1527. https://doi.org/10.1016/j.dsr2.2007.05.010

912   Lüke, C., Speth, D. R., Kox, M. A. R., Villanueva, L., & Jetten, M. S. M. (2016). Metagenomic
913   analysis of nitrogen and methane cycling in the Arabian Sea oxygen minimum zone. *PeerJ*, *4*,
914   e1924. https://doi.org/10.7717/peerj.1924

915   Luo, G., Algeo, T. J., Huang, J., Zhou, W., Wang, Y., Yang, H., et al. (2014). Vertical $\delta^{13}C_{org}$
916   gradients record changes in planktonic microbial community composition during the end-
917   Permian mass extinction. *Palaeogeography, Palaeoclimatology, Palaeoecology*, *396*, 119–131.
918   https://doi.org/10.1016/j.palaeo.2014.01.006

919   Matys, E. D., Sepúlveda, J., Pantoja, S., Lange, C. B., Caniupán, M., Lamy, F., & Summons, R.
920   E. (2017). Bacteriohopanepolyols along redox gradients in the Humboldt Current System off
921   northern Chile. *Geobiology*, *15*(6), 844–857. https://doi.org/10.1111/gbi.12250

922   Meyers, P. A. (2014). Why are the $\delta^{13}C_{org}$ values in Phanerozoic black shales more negative
923   than in modern marine organic matter? *Geochemistry, Geophysics, Geosystems*, *15*(7), 3085–
924   3106. https://doi.org/10.1002/2014GC005305

925   Meyers, P. A., & Arnaboldi, M. (2008). Paleoceanographic implications of nitrogen and organic
926   carbon isotopic excursions in mid-Pleistocene sapropels from the Tyrrhenian and Levantine
927   Basins, Mediterranean Sea. *Palaeogeography, Palaeoclimatology, Palaeoecology*, *266*(1), 112–
928   118. https://doi.org/10.1016/j.palaeo.2008.03.018

929   Middelburg, J. J. (1989). A simple rate model for organic matter decomposition in marine
930   sediments. *Geochimica et Cosmochimica Acta*, *53*(7), 1577–1581. https://doi.org/10.1016/0016-
931   7037(89)90239-1

932   Middelburg, J. J., Vlug, T., Jaco, F., & van der Nat, W. A. (1993). Organic matter mineralization
933   in marine systems. *Global and Planetary Change*, *8*(1), 47–58. https://doi.org/10.1016/0921-
934   8181(93)90062-S

935   Middelburg J. J. (2011). Chemoautotrophy in the ocean. *Geophysical Research Letters*, *38*(24).
936   https://doi.org/10.1029/2011GL049725

937   Moos, C. (2000). *Reconstruction of upwelling intensity and paleo-nutrient gradients in the*
938   *Northwest Arabian Sea derived from stable carbon and oxygen isotopes of planktic foraminifera*.
939   University of Bremen, Bremen, Germany. Retrieved from http://elib.suub.uni-
940   bremen.de/ip/docs/00010276.pdf

941   Naqvi, S. W. A., & Shailaja, M. S. (1993). Activity of the respiratory electron transport system
942   and respiration rates within the oxygen minimum layer of the Arabian Sea. *Deep Sea Research*
943   *Part II: Topical Studies in Oceanography, 40*(3), 687–695. https://doi.org/10.1016/0967-
944   0645(93)90052-O

945   Nierop, K. G. J., Reichart, G.-J., Veld, H., & Sinninghe Damsté, J. S. (2017). The influence of
946   oxygen exposure time on the composition of macromolecular organic matter as revealed by
947   surface sediments on the Murray Ridge (Arabian Sea). *Geochimica et Cosmochimica Acta*, *206*,
948   40–56. https://doi.org/10.1016/j.gca.2017.02.032

949   Pachiadaki, M. G., Sintes, E., Bergauer, K., Brown, J. M., Record, N. R., Swan, B. K., et al.
950   (2017). Major role of nitrite-oxidizing bacteria in dark ocean carbon fixation. *Science*,
951   *358*(6366), 1046–1051. https://doi.org/10.1126/science.aan8260

952   Pagani, M. (2005). Marked Decline in Atmospheric Carbon Dioxide Concentrations During the
953   Paleogene. *Science*, *309*(5734), 600–603. https://doi.org/10.1126/science.1110063

954   Pancost, R. D., & Pagani, M. (2005). Controls on the Carbon Isotopic Compositions of Lipids in
955   Marine Environments. In *Marine Organic Matter: Biomarkers, Isotopes and DNA* (pp. 209–
956   249). Springer, Berlin, Heidelberg. https://doi.org/10.1007/698_2_007
957
958   Pancost, R. D., & Sinninghe Damsté, J. S. (2003). Carbon isotopic compositions of prokaryotic
959   lipids as tracers of carbon cycling in diverse settings. *Chemical Geology*, *195*(1–4), 29–58.
960   https://doi.org/10.1016/S0009-2541(02)00387-X

961   Pancost, R. D., Freeman, K. H., & Patzkowsky, M. E. (1999). Organic-matter source variation
962   and the expression of a late Middle Ordovician carbon isotope excursion. *Geology*, *27*(11),
963   1015–1018. https://doi.org/10.1130/0091-7613(1999)027<1015:OMSVAT>2.3.CO;2

964   Pancost, R. D., Steart, D. S., Handley, L., Collinson, M. E., Hooker, J. J., Scott, A. C., et al.
965   (2007). Increased terrestrial methane cycling at the Palaeocene–Eocene thermal maximum.
966   *Nature*, *449*(7160), 332–335. https://doi.org/10.1038/nature06012

967 Pancost, R. D., Freeman, K. H., Herrmann, A. D., Patzkowsky, M. E., Ainsaar, L., & Martma, T.
968 (2013). Reconstructing Late Ordovician carbon cycle variations. *Geochimica et Cosmochimica*
969 *Acta*, *105*, 433–454. https://doi.org/10.1016/j.gca.2012.11.033

970 Parnell, A. C., Inger, R., Bearhop, S., & Jackson, A. L. (2010). Source Partitioning Using Stable
971 Isotopes: Coping with Too Much Variation. *PLOS ONE, 5*(3), e9672.
972 https://doi.org/10.1371/journal.pone.0009672

973 Paulmier, A., & Ruiz-Pino, D. (2009). Oxygen minimum zones (OMZs) in the modern ocean.
974 *Progress in Oceanography, 80*(3–4), 113–128. https://doi.org/10.1016/j.pocean.2008.08.001

975 Pearson, A. (2010). Pathways of Carbon Assimilation and Their Impact on Organic Matter
976 Values δ13C. In K. N. Timmis (Ed.), *Handbook of Hydrocarbon and Lipid Microbiology* (pp.
977 143–156). Berlin, Heidelberg: Springer Berlin Heidelberg. Retrieved from
978 http://link.springer.com/10.1007/978-3-540-77587-4_9

979 Pearson, Ann, & Rusch, D. B. (2009). Distribution of microbial terpenoid lipid cyclases in the
980 global ocean metagenome. *The ISME Journal*, *3*(3), 352–363.
981 https://doi.org/10.1038/ismej.2008.116

982 Phillips, D. L., Newsome, S. D., & Gregg, J. W. (2005). Combining sources in stable isotope
983 mixing models: alternative methods. *Oecologia*, *144*(4), 520–527.
984 https://doi.org/10.1007/s00442-004-1816-8

985 Pitcher, A., Villanueva, L., Hopmans, E. C., Schouten, S., Reichart, G.-J., & Sinninghe Damsté,
986 J. S. (2011). Niche segregation of ammonia-oxidizing archaea and anammox bacteria in the
987 Arabian Sea oxygen minimum zone. *The ISME Journal*, *5*(12), 1896–1904.
988 https://doi.org/10.1038/ismej.2011.60

989 Pozzato, L., Oevelen, D. V., Moodley, L., Soetaert, K., & Middelburg, J. J. (2013a). Sink or
990 link? The bacterial role in benthic carbon cycling in the Arabian Sea's oxygen minimum zone.
991 *Biogeosciences*, *10*(11), 6879–6891. https://doi.org/10.5194/bg-10-6879-2013

992 Pozzato, Lara, van Oevelen, D., Moodley, L., Soetaert, K., & Middelburg, J. J. (2013b). Carbon
993 processing at the deep-sea floor of the Arabian Sea oxygen minimum zone: A tracer approach.
994 *Journal of Sea Research*, *78*, 45–58. https://doi.org/10.1016/j.seares.2013.01.002

995 Queste, B. Y., Vic, C., Heywood, K. J., & Piontkovski, S. A. (2018). Physical Controls on
996 Oxygen Distribution and Denitrification Potential in the North West Arabian Sea. *Geophysical*
997 *Research Letters*, *45*(9), 4143–4152. https://doi.org/10.1029/2017GL076666

998 Reinthaler, T., van Aken, H. M., & Herndl, G. J. (2010). Major contribution of autotrophy to
999 microbial carbon cycling in the deep North Atlantic's interior. *Deep Sea Research Part II:*
1000 *Topical Studies in Oceanography*, *57*(16), 1572–1580.
1001 https://doi.org/10.1016/j.dsr2.2010.02.023

Rixen, T., & Ittekkot, V. (2005). Nitrogen deficits in the Arabian Sea, implications from a three component mixing analysis. *Deep Sea Research Part II: Topical Studies in Oceanography*, *52*(14–15), 1879–1891. https://doi.org/10.1016/j.dsr2.2005.06.007

Roullier, F., Berline, L., Guidi, L., Durrieu De Madron, X., Picheral, M., Sciandra, A., et al. (2014). Particle size distribution and estimated carbon flux across the Arabian Sea oxygen minimum zone. *Biogeosciences*, *11*(16), 4541–4557. https://doi.org/10.5194/bg-11-4541-2014

Rush, D., & Sinninghe Damsté, J. S. (2017). Lipids as paleomarkers to constrain the marine nitrogen cycle: Lipids as paleomarkers. *Environmental Microbiology*, *19*(6), 2119–2132. https://doi.org/10.1111/1462-2920.13682

Rush, D., Sinninghe Damsté, J. S., Poulton, S. W., Thamdrup, B., Garside, A. L., Acuña González, J., et al. (2014). Anaerobic ammonium-oxidising bacteria: A biological source of the bacteriohopanetetrol stereoisomer in marine sediments. *Geochimica et Cosmochimica Acta*, *140*, 50–64. https://doi.org/10.1016/j.gca.2014.05.014

Rush, D., Talbot, H. M., Meer, M. T. J. van der, Hopmans, E. C., Douglas, B., & Sinninghe Damsté, J. S. (2019). Biomarker evidence for the occurrence of anaerobic ammonium oxidation in the eastern Mediterranean Sea during Quaternary and Pliocene sapropel formation. *Biogeosciences Discussions*, 1–27. https://doi.org/10.5194/bg-2019-27

Sáenz, J. P., Wakeham, S. G., Eglinton, T. I., & Summons, R. E. (2011). New constraints on the provenance of hopanoids in the marine geologic record: Bacteriohopanepolyols in marine suboxic and anoxic environments. *Organic Geochemistry*, *42*(11), 1351–1362. https://doi.org/10.1016/j.orggeochem.2011.08.016

Sakata, S., Hayes, J. M., McTaggart, A. R., Evans, R. A., Leckrone, K. J., & Togasaki, R. K. (1997). Carbon isotopic fractionation associated with lipid biosynthesis by a cyanobacterium: Relevance for interpretation of biomarker records. *Geochimica et Cosmochimica Acta*, *61*(24), 5379–5389. https://doi.org/10.1016/S0016-7037(97)00314-1

Schenau, S. J., Passier, H. F., Reichart, G. J., & de Lange, G. J. (2002). Sedimentary pyrite formation in the Arabian Sea. *Marine Geology*, *185*(3), 393–402. https://doi.org/10.1016/S0025-3227(02)00183-4

Schlitzer, R. (2002). Carbon export fluxes in the Southern Ocean: results from inverse modeling and comparison with satellite-based estimates. *Deep Sea Research Part II: Topical Studies in Oceanography*, *49*(9), 1623–1644. https://doi.org/10.1016/S0967-0645(02)00004-8

Schmaljohann, R., Drews, M., Walter, S., Linke, P., Rad, U. von, & Imhoff, J. F. (2001). Oxygen-minimum zone sediments in the northeastern Arabian Sea off Pakistan: a habitat for the bacterium Thioploca. *Marine Ecology Progress Series*, *211*, 27–42. https://doi.org/10.3354/meps211027

1037 Schmidtko, S., Stramma, L., & Visbeck, M. (2017). Decline in global oceanic oxygen content
1038 during the past five decades. *Nature*, *542*(7641), 335–339. https://doi.org/10.1038/nature21399

1039 Schouten, S., Strous, M., Kuypers, M. M. M., Rijpstra, W. I. C., Baas, M., Schubert, C. J., et al.
1040 (2004). Stable Carbon Isotopic Fractionations Associated with Inorganic Carbon Fixation by
1041 Anaerobic Ammonium-Oxidizing Bacteria. *Applied and Environmental Microbiology*, *70*(6),
1042 3785–3788. https://doi.org/10.1128/AEM.70.6.3785-3788.2004

1043 Schouten, Stefan, Klein Breteler, W. C. M., Blokker, P., Schogt, N., Rijpstra, W. I. C., Grice, K.,
1044 et al. (1998). Biosynthetic effects on the stable carbon isotopic compositions of algal lipids:
1045 implications for deciphering the carbon isotopic biomarker record. *Geochimica et Cosmochimica*
1046 *Acta*, *62*(8), 1397–1406. https://doi.org/10.1016/S0016-7037(98)00076-3

1047 Schouten, Stefan, Hoefs, M. J. L., & Sinninghe Damsté, J. S. (2000). A molecular and stable
1048 carbon isotopic study of lipids in late Quaternary sediments from the Arabian Sea. *Organic*
1049 *Geochemistry*, *31*(6), 509–521. https://doi.org/10.1016/S0146-6380(00)00031-0

1050 Schouten, Stefan, Pitcher, A., Hopmans, E. C., Villanueva, L., van Bleijswijk, J., & Sinninghe
1051 Damsté, J. S. (2012). Intact polar and core glycerol dibiphytanyl glycerol tetraether lipids in the
1052 Arabian Sea oxygen minimum zone: I. Selective preservation and degradation in the water
1053 column and consequences for the TEX86. *Geochimica et Cosmochimica Acta*, *98*, 228–243.
1054 https://doi.org/10.1016/j.gca.2012.05.002

1055 Sessions, A. L., Zhang, L., Welander, P. V., Doughty, D., Summons, R. E., & Newman, D. K.
1056 (2013). Identification and quantification of polyfunctionalized hopanoids by high temperature
1057 gas chromatography–mass spectrometry. *Organic Geochemistry*, *56*, 120–130.
1058 https://doi.org/10.1016/j.orggeochem.2012.12.009

1059 Shaffer, G., Olsen, S. M., & Pedersen, J. O. P. (2009). Long-term ocean oxygen depletion in
1060 response to carbon dioxide emissions from fossil fuels. *Nature Geoscience*, *2*(2), 105–109.
1061 https://doi.org/10.1038/ngeo420

1062 Sokoll, S., Holtappels, M., Lam, P., Collins, G., Schlüter, M., Lavik, G., & Kuypers, M. M. M.
1063 (2012). Benthic Nitrogen Loss in the Arabian Sea Off Pakistan. *Frontiers in Microbiology*, *3*.
1064 https://doi.org/10.3389/fmicb.2012.00395

1065 Spiker, E. C., & Hatcher, P. G. (1987). The effects of early diagenesis on the chemical and stable
1066 carbon isotopic composition of wood. *Geochimica et Cosmochimica Acta*, *51*(6), 1385–1391.
1067 https://doi.org/10.1016/0016-7037(87)90323-1

1068 Stramma, L., Schmidtko, S., Levin, L. A., & Johnson, G. C. (2010). Ocean oxygen minima
1069 expansions and their biological impacts. *Deep Sea Research Part I: Oceanographic Research*
1070 *Papers*, *57*(4), 587–595. https://doi.org/10.1016/j.dsr.2010.01.005

1071 Strous, M., Kuenen, J. G., & Jetten, M. S. M. (1999). Key Physiology of Anaerobic Ammonium
1072 Oxidation. *Applied and Environmental Microbiology*, *65*(7), 3248–3250.

1073 Talbot, H. M., Rohmer, M., & Farrimond, P. (2007). Rapid structural elucidation of composite
1074 bacterial hopanoids by atmospheric pressure chemical ionization liquid chromatography/ion trap
1075 mass spectrometry. *Rapid Communications in Mass Spectrometry*, *21*(6), 880–892.
1076 https://doi.org/10.1002/rcm.2911

1077 Taylor, G. T., Iabichella, M., Ho, T.-Y., Scranton, M. I., Thunell, R. C., Muller-Karger, F., &
1078 Varela, R. (2001). Chemoautotrophy in the redox transition zone of the Cariaco Basin: A
1079 significant midwater source of organic carbon production. *Limnology and Oceanography*, *46*(1),
1080 148–163. https://doi.org/10.4319/lo.2001.46.1.0148

1081 Ulloa, O., Canfield, D. E., DeLong, E. F., Letelier, R. M., & Stewart, F. J. (2012). Microbial
1082 oceanography of anoxic oxygen minimum zones. *Proceedings of the National Academy of
1083 Sciences of the United States of America*, *109*(40), 15996–16003.
1084 https://doi.org/10.1073/pnas.1205009109

1085 Van Kaam-Peters, H. M. E., Schouten, S., Köster, J., & Sinninghe Damstè, J. S. (1998). Controls
1086 on the molecular and carbon isotopic composition of organic matter deposited in a
1087 Kimmeridgian euxinic shelf sea: evidence for preservation of carbohydrates through
1088 sulfurization. *Geochimica et Cosmochimica Acta*, *62*(19), 3259–3283.
1089 https://doi.org/10.1016/S0016-7037(98)00231-2

1090 Villanueva, L., Speth, D. R., Vanalen, T., Hoischen, A., & Jetten, M. (2014). Shotgun
1091 metagenomic data reveals significant abundance but low diversity of "Candidatus Scalindua"
1092 marine anammox bacteria in the Arabian Sea oxygen minimum zone. *Frontiers in Microbiology*,
1093 *5*. https://doi.org/10.3389/fmicb.2014.00031

1094 van de Vossenberg, J., Rattray, J. E., Geerts, W., Kartal, B., Niftrik, L. V., Donselaar, E. G. V.,
1095 et al. (2008). Enrichment and characterization of marine anammox bacteria associated with
1096 global nitrogen gas production. *Environmental Microbiology*, *10*(11), 3120–3129.
1097 https://doi.org/10.1111/j.1462-2920.2008.01643.x

1098 van de Vossenberg, J., Woebken, D., Maalcke, W. J., Wessels, H. J. C. T., Dutilh, B. E., Kartal,
1099 B., et al. (2013). The metagenome of the marine anammox bacterium '*Candidatus* Scalindua
1100 profunda' illustrates the versatility of this globally important nitrogen cycle bacterium.
1101 *Environmental Microbiology*, *15*(5), 1275–1289. https://doi.org/10.1111/j.1462-
1102 2920.2012.02774.x

1103 Wakeham, S. G., & McNichol, A. P. (2014). Transfer of organic carbon through marine water
1104 columns to sediments – insights from stable and radiocarbon isotopes of lipid biomarkers.
1105 *Biogeosciences*, *11*(23), 6895–6914. https://doi.org/10.5194/bg-11-6895-2014

1106 Wakeham, Stuart G., Peterson, M. L., Hedges, J. I., & Lee, C. (2002). Lipid biomarker fluxes in
1107 the Arabian Sea, with a comparison to the equatorial Pacific Ocean. *Deep Sea Research Part II:
1108 Topical Studies in Oceanography*, *49*(12), 2265–2301. https://doi.org/10.1016/S0967-
1109 0645(02)00037-1

1110 Ward, B. B., Devol, A. H., Rich, J. J., Chang, B. X., Bulow, S. E., Naik, H., et al. (2009).
1111 Denitrification as the dominant nitrogen loss process in the Arabian Sea. *Nature*, *461*(7260), 78–
1112 81. https://doi.org/10.1038/nature08276

1113 van Winden, J. F., Talbot, H. M., Kip, N., Reichart, G.-J., Pol, A., McNamara, N. P., et al.
1114 (2012). Bacteriohopanepolyol signatures as markers for methanotrophic bacteria in peat moss.
1115 *Geochimica et Cosmochimica Acta*, *77*, 52–61. https://doi.org/10.1016/j.gca.2011.10.026

1116 Witkowski, C. R., Weijers, J. W. H., Blais, B., Schouten, S., & Damsté, J. S. S. (2018).
1117 Molecular fossils from phytoplankton reveal secular pCO$_2$ trend over the Phanerozoic. *Science*
1118 *Advances*, *4*(11), eaat4556. https://doi.org/10.1126/sciadv.aat4556

1119 Wright, J. J., Konwar, K. M., & Hallam, S. J. (2012). Microbial ecology of expanding oxygen
1120 minimum zones. *Nature Reviews Microbiology*, *10*(6), 381–394.
1121 https://doi.org/10.1038/nrmicro2778

1122 Wuchter, C. (2006). Archaeal nitrification in the ocean. *Proceedings of the National Academy of*
1123 *Sciences*, *103*(33), 12317–12322. https://doi.org/10.1073/pnas.0600756103

1124 Zachos, J. C., Röhl, U., Schellenberg, S. A., Sluijs, A., Hodell, D. A., Kelly, D. C., et al. (2005).
1125 Rapid Acidification of the Ocean During the Paleocene-Eocene Thermal Maximum. *Science*,
1126 *308*(5728), 1611–1615. https://doi.org/10.1126/science.1109004

1127 Zhang, C. L., Huang, Z., Cantu, J., Pancost, R. D., Brigmon, R. L., Lyons, T. W., & Sassen, R.
1128 (2005). Lipid Biomarkers and Carbon Isotope Signatures of a Microbial (Beggiatoa) Mat
1129 Associated with Gas Hydrates in the Gulf of Mexico. *Applied and Environmental Microbiology*,
1130 *71*(4), 2106–2112. https://doi.org/10.1128/AEM.71.4.2106-2112.2005

1131 Ziegler, M., Jilbert, T., de Lange, G. J., Lourens, L. J., & Reichart, G.-J. (2008). Bromine counts
1132 from XRF scanning as an estimate of the marine organic carbon content of sediment cores:
1133 Bromine as estimator for sediment composition. *Geochemistry, Geophysics, Geosystems*, *9*(5).
1134 https://doi.org/10.1029/2007GC001932
1135
1136
1137
1138
1139
1140
1141
1142
1143
1144
1145

1146

1147 **Table 1.** $\delta^{13}C$ values of analysed samples. s.d. = standard deviation of three repeat analyses, n.d.
1148 = not determined (single analysis). The values shown are natural abundance from unamended
1149 cores, and from incubations with ^{13}C labelled DOM and POM, under oxic and suboxic
1150 conditions. * indicates outliers (Grubbs).

		$\delta^{13}C$ value [‰ V-PDB]				
Type	**Sample**	**BHT**	**s.d.**	**BHT'**	**s.d.**	**C_{org}**
Biomass	Scalindua sp.	-47.8	1	-47.6	1	
Arabian Sea Natural abundance	P900 - 1 cm	-24.7	1.3	-39.1	1.3	-21.5
	P900 - 3 cm	-27.0	1.4	-48.1	1.1	
	P900 - 7 cm	-26.1	0.4	-41.4	0.5	
	P1800 - 1 cm	-25.1	1.7	-48.1	1.6	-20.3
	P1800 - 3 cm	-28.8	2.1	-46.6	4.1	
	P1800 - 7 cm	-27.1	0.6	-45.5	1.0	
Arabian Sea Incubations	P900, suboxic, DOM - 1 cm	-27.9	n.d.	-45.9	n.d.	
	P900, suboxic, DOM - 3 cm	-26.6	n.d.	-42.0	n.d.	
	P900, suboxic, POM - 1 cm	-41.6*	n.d.	-75.2*	n.d.	
	P900, suboxic, POM - 3 cm	-26.4	n.d.	-49.8	n.d.	
	P900, oxic, POM - 1 cm	-27.1	n.d.	-51.5	n.d.	
	P900, oxic, POM - 3 cm	-25.2	n.d.	-47.8	n.d.	
	P1800, oxic, DOM - 1 cm	-21.3	n.d.	-42.0	n.d.	
	P1800, oxic, DOM - 3 cm	-28.3	n.d.	-45.6	n.d.	
	P1800, suboxic, POM - 1 cm	-52.2*	n.d.	-101.9*	n.d.	
	P1800, suboxic, POM - 3 cm	-28.8	n.d.	-47.1	n.d.	
	P1800, oxic, POM - 1 cm	-30.2	n.d.	-51.3	n.d.	
	P1800, oxic, POM - 3 cm	-28.0	n.d.	-46.1	n.d.	

1151